6.13 Greenhouse Climates

M Pagani, Yale University, New Haven, CT, USA
M Huber, Purdue University, West Lafayette, IN, USA
B Sageman, Northwestern University, Evanston, IL, USA

6.13.1 Introduction

The state of Earth's climate, viewed dimly through bits of dirt and bone, appears to have waxed and waned, shifted and flipped, since the start of its long history. Celestial, tectonic, and biological forces leave nothing untouched, perpetually pushing the internal variability of climate this way and that, and sometimes over the edge. A wide range of periodic and quasi-periodic changes in physical sedimentation, biological processes, chemical reactions, and atmospheric effects, have been surmised and detected, forced by both allochthonous and autochthonous beats. The notion promoted by Al Fischer, of long 30–36 Ma cycles (Dorman, 1968; Fischer and Arthur, 1977) riding on 300 Ma supercycles (Fischer and Arthur, 1977), expressed a world responding to changes in atmospheric carbon dioxide concentration and toggling between dominant 'greenhouse' and 'icehouse' states (Fischer, 1981, 1982; Frakes et al., 1992) that was reflected in marine and terrestrial diversity, ocean structure, marine redox conditions, carbonate saturation, and extent of glaciation. Long-term changes in climate were assumed driven by carbon dioxide concentration (Chamberlin, 1899) – a view consistent with some of the first estimates of climate sensitivity to CO_2 (Arrhenius, 1896; Plass, 1956), and one that can now be tested as improved methods of quantifying ancient carbon dioxide concentrations.

Greenhouse climates, which lack substantial accumulations of permanent continental ice because of temperatures much warmer than the Holocene average, are the common condition for the past 540 Ma. Cold, glacial conditions characteristic of our modern Earth are unusual. But greenhouse climates are also characterized by a pervasive variability that appears sensitive to both internal drivers and external (i.e., orbital) variations, and can be characterized by abrupt climate shifts, indicative of either thresholds in the climate system, strongly nonlinear interactions, or sudden changes in climatic forcing factors. One of the major objectives of climate science is to understand these dynamics and ultimately improve our ability to predict future climate change. The investigation of greenhouse climates is making substantial progress toward this goal, driven by innovations in paleoenvironmental reconstructions for both marine and terrestrial realms, and by significant improvements in paleoclimate modeling. Paleotemperature proxies, including carbonate oxygen isotopic compositions and Mg/Ca ratios, and other methods that might still be considered works-in-progress, such as $U^{K'}_{37}$, TEX_{86}, and clumped isotopes, are now complimented by new proxy reconstructions of atmospheric CO_2 that allow us to address the long-standing challenge of constraining climate sensitivity to greenhouse gas forcing.

For this work, we review proxy records and modeling studies for the most recent greenhouse climate state and present a broad overview of our evolving perspectives including the primary agents forcing global climate and the feedbacks responsible for the observed temperature distributions.

6.13.2 Temperatures: An Evolving Perspective

In this review, greenhouse climates are considered to be intervals too warm to sustain substantial continental glaciation. By this definition, the last major greenhouse interval persisted from the late Permian, ~260 Ma ago (Montañez and Poulsen, 2013), to the Eocene/Oligocene boundary (~35 Ma ago). Because so much more is known about the climates of the Cretaceous and early Cenozoic from proxy records and modeling studies, we restrict our discussion to these intervals of time.

The Cretaceous has long been recognized for its unusual warmth (Hallam, 1985; Urey et al., 1951). Climatic history gleaned from some of the first oxygen isotope measurements

($\delta^{18}O$) of belemnites, brachiopods, inoceramids, and oysters, show a broad multimillion-year temperature rise-and-fall from the Albian through the Maastrichtian, with peak temperatures near the early Campanian (Lowenstam and Epstein, 1954). Subsequent isotope analyses of foraminifera (Douglas and Savin, 1973, 1975; Savin, 1977; Savin et al., 1975; Shackleton and Kennett, 1975) and bivalves (Dorman, 1966) extended the appearance of very warm ocean temperature records through the early Cenozoic, but with another peak in temperature sometime during the Eocene followed by a long decline and precipitous drops in temperature toward our modern icehouse state. Although cautiously quantitative, these earliest isotope measurements imply much warmer temperatures for the Cretaceous and Eocene, revealing a distinctly unique view of ancient climate – a world with an expanded tropical realm unlikely to support 'permanent' polar ice sheets (i.e., those with durations in excess of millions of years).

Terrestrial temperature estimates, inferred from leaf margin analysis and the composition of fossil floras, also imply warm climates throughout the Cretaceous and early Eocene (Askin, 1990; Axelrod, 1984; Kowalski and Dilcher, 2002; Poole et al., 2005; Uhl et al., 2007a,b; Wolfe, 1978, 1994). Fossil floras from the North Slope of Alaska (Parrish and Spicer, 1988; Spicer and Parrish, 1986) and northeastern Russia (Spicer et al., 2002) indicate that high Arctic mean annual temperature (MAT) fell from ~13 °C in the mid-Cretaceous (Herman and Spicer, 1996; Spicer et al., 2002) to 2–8 °C by the Maastrichtian in areas that currently have MAT of −14 °C (Spicer et al., 2008). Warm polar regions with winter temperatures above freezing are also inferred from the occurrence of fossil crocodilians and other aquatic vertebrates at mid- to high latitudes during the Cretaceous (Markwick, 1998, 2007; Tarduno et al., 1998). The recent discovery of Late Cretaceous frost-intolerant floras in the remote interior of Siberia far from ameliorating effects of the ocean, allows a MAT reconstruction of ~12 °C, which is 10 °C warmer than model simulations (Spicer et al., 2008).

Oxygen isotope compositions of carbonates have been broadly applied to constrain MAT and meridional-temperature gradients. From the start, the role of diagenetic alteration and selective preservation in producing anomalously cool tropical temperatures was a leading issue in the minds of researchers (Savin et al., 1975). But even corrections for temperature biases resulting from diagenetic alteration resulted in the appearance of relatively cool tropical SSTs (i.e., tropical temperatures similar to or colder than today with much warmer temperatures poleward) during the Cretaceous (Barron, 1983; Crowley and Zachos, 2000) (**Figure 1**).

The earliest attempts to model Cretaceous temperatures resulted in a poor fit with proxy data and suggested that cool tropical SSTs inferred from oxygen isotopes needed to be re-evaluated (Barron et al., 1981; Crowley and Zachos, 2000; Poulsen et al., 1999; Saltzman and Barron, 1982). Suspicions of spurious temperature estimates (Savin et al., 1975) were largely ignored, and the resulting combination of a cool tropical realm (as much as 6.5 °C cooler than today; D'Hondt and Arthur, 1996) occurring with extraordinarily warm high latitudes (D'Hondt and Arthur, 1996; Huber et al., 1995; Sellwood et al., 1994) spawned novel modeling exercises to explain the apparent phenomena. This led some to conclude that the climate system alters its meridional-temperature

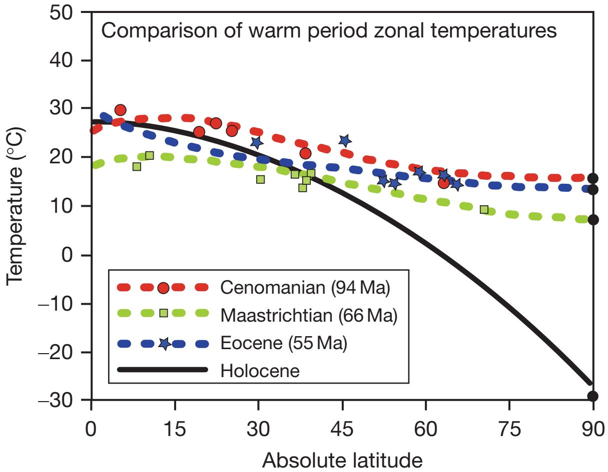

Figure 1 Zonal sea-surface temperature profiles based on $\delta^{18}O$ values of carbonates that were likely diagenetically altered (modified from Crowley T and Zachos JC (2000) Comparison of zonal temperature profiles for past warm time periods. In: Huber BT, MacLeod KG, and Wing SL (eds.) *Warm Climates in Earth History*, pp. 50–766. Cambridge: Cambridge University Press). Polar temperatures (black filled circles) are based on benthic foraminiferal $\delta^{18}O$ values. These temperatures are no longer considered valid.

gradient in such a way as to minimize global mean-temperature change and implied a very small or even zero climate sensitivity to forcing (Lindzen, 1993, 1994, 1997; Lindzen and Farrell, 1977; Sun and Lindzen, 1993). However, we now recognize that many of the cool tropical temperature estimates derived from oxygen isotope measurements of Cretaceous and Eocene fossils reflect diagenetic cements and recrystallization that promote cooler temperature estimates, particularly for warm tropical surface-waters (**Figure 1**), to far greater extent than initially assumed (Bice et al., 2006; Head et al., 2009; Huber, 2009; Huber and Sloan, 2000; Norris et al., 2002; Pearson et al., 2001; Schrag, 1999). It is now well accepted that tropical greenhouse temperatures were warmer than modern values, but the degree to which previous reconstructions were cold-biased has only been fully appreciated in the past decade.

6.13.2.1 A New Generation of Temperature Proxy Records

Isotopic and elemental ratio evidence for substantial low-latitude warming during the most recent greenhouse interval is increasingly apparent (Bice et al., 2003, 2006; Huber, 1998; Norris and Wilson, 1998). Temperature estimates from $\delta^{18}O$ and Mg/Ca values of extremely well-preserved surface-dwelling foraminifera have raised tropical to subtropical temperatures for the middle- (Bornemann et al., 2008; Clarke and Jenkyns, 1999; Norris and Wilson, 1998; Norris et al., 2002; Wilson and Norris, 2001; Wilson et al., 2002) to late Cretaceous (Pearson et al., 2001; Wilson and Opdyke, 1996) and early-to-middle Eocene (Pearson et al., 2001, 2007; Sexton et al., 2006; Tripati et al., 2003) to 30–37 °C – significantly higher than modern, but large uncertainties in absolute values remain (Huber, 2008). For example, foraminiferal oxygen isotopic compositions are affected by ocean pH and its influence on the proportion of HCO_3^-/CO_3^{2-}, and ultimately, the thermodynamic distribution of oxygen isotopes among carbonate species (Spero et al., 1997; Zeebe, 1999). Higher CO_2 concentrations and subsequently lower seawater pH leads to a greater isotopic fractionation between water and carbonate (Zeebe, 1999). As a result, if atmospheric CO_2 concentrations are roughly as high as geochemical models predict (3–8 times modern values with resulting seawater pH values of 7.9–7.7), it is likely that even the best-preserved Cretaceous carbonates express minimum estimates, with an excess of 2–3.5 °C hidden in isotope effects (Zeebe, 2001). Further, accurate temperature and gradient assessments require knowledge of the oxygen isotopic composition of shallow seawater ($\delta^{18}O_{sw}$) on the regional scale, given the importance of spatial variability in precipitation and evaporation, potential riverine inputs, and watermass transport by the ocean circulation. Simulations of $\delta^{18}O_{sw}$ during greenhouse conditions suggest significant and differential errors in zonal temperature reconstructions if not properly taken into account (Poulsen et al., 1999; Roberts et al., 2009; Roche et al., 2006; Tindall et al., 2010; Zachos et al., 1994; Zhou et al., 2008).

The advent of the new organic temperature proxy TEX_{86} has also pushed SST estimates higher. The TEX_{86} proxy is founded on the distribution of the membrane lipids of marine Thaumarchaeota – isoprenoid glycerol dibiphytanyl glycerol tetraethers (i.e., GDGTs) (Schouten et al., 2002). Ratios of GDGTs that vary in the number of cyclopentane moieties have been calibrated to sea-surface temperatures in the modern ocean with an uncertainty of as much as $\sim\pm4$ °C (Kim et al., 2008, 2010; Liu et al., 2009; Schouten et al., 2002, 2003). TEX_{86} data suggest early- (Dumitresc et al., 2006; Jenkyns et al., 2012; Littler et al., 2011) to middle Cretaceous tropical conditions (Forster et al., 2007a,b; Schouten et al., 2003) of 32–36 °C to over 45 °C depending on which version of the TEX_{86} temperature calibration (Kim et al., 2010) is applied. Mid- to high-latitude temperatures during the early (Littler et al., 2011) and late Cretaceous (Jenkyns et al., 2004) also appear much warmer viewed through this proxy lens.

The accumulated data support an evolution of temperature from a cooler (although still warm compared to modern) early Cretaceous to peak warming by the Turonian (~90–94 Ma) and returning to cooler temperatures by latest Cretaceous (Barrera et al., 1987; Davies et al., 2009; Friedrich et al., 2012; Pirrie and Marshall, 1990; Wilf, 2000) and early Paleocene (Wilf, 2000; Zachos et al., 2001) (**Figure 2**). Cooler conditions gave way to a trend of rising global temperatures that eventually peaked in the early Eocene (Cramer et al., 2009). Carbonate isotope records (Friedrich et al., 2012; Hollis et al., 2009; Zachos et al., 2001, 2006), distribution of vegetation (Basinger et al., 1994; Greenwood and Wing, 1995; Wilf et al., 2003), and reptile fossils (Eberle and Greenwood, 2012; Estes and Hutchison, 1980; Hutchinson, 1982; Markwick, 2007), as well as recent TEX_{86} values (Brinkhuis et al., 2006; Creech et al., 2010; Hollis et al., 2009; Sluijs et al., 2006; Zachos et al., 2006) indicate a very warm early Eocene (55–48 Ma), particularly at high latitudes, although probably cooler than the extraordinary warmth of the middle Cretaceous (Friedrich et al., 2012).

Continental annual-mean and winter temperatures during the early Eocene were clearly warmer than modern conditions, with greatly reduced meridional-temperature gradients (Greenwood and Wing, 1995; Wolfe, 1994). At times, crocodiles (Hutchinson, 1982), tapir-like mammals (Eberle, 2005), and palm trees (Sluijs et al., 2009) flourished around the Arctic Ocean with warm, sometimes brackish surface waters (Brinkhuis et al., 2006; Speelman et al., 2009). Ocean bottom-water temperatures, inferred from oxygen isotope or Mg/Ca compositions of benthic foraminifera were ~10–12 °C higher than modern values (Cramer et al., 2009; Lear et al., 2000; Miller et al., 1987; Zachos et al., 1994), implying that deep-water source regions experienced winter temperatures well above freezing. Recent palynological results from Antarctica during peak warming of the Eocene show thermophyllic flora with containing palms and Bombacoideae – clear evidence that winter temperatures were well above freezing (Pross et al., 2012).

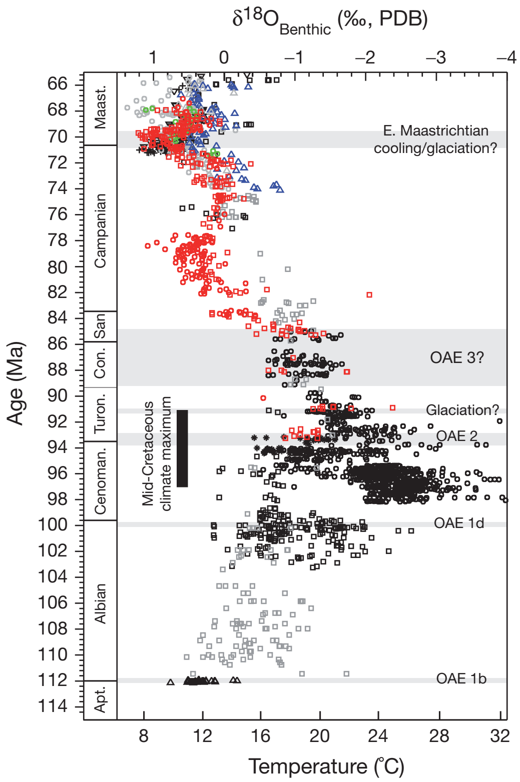

Figure 2 Stable oxygen isotope compilation of Cretaceous benthic foraminifera (modified from Friedrich O, Norris RD, and Erbacher J (2012) Evolution of middle to Late Cretaceous oceans – A 55 m.y. record of Earth's temperature and carbon cycle. *Geology* 40: 107–110). *Black symbols* represent North Atlantic Ocean, *gray symbols*; southern high latitudes, *red symbols*; Pacific Ocean, *blue symbols*; subtropical South Atlantic Ocean, *green symbols*; Indian Ocean. OAE, oceanic anoxic event. Some of the data derive from exceptionally well-preserved (glassy) foraminiferal tests from the western equatorial Atlantic at Demerara Rise (Friedrich et al., 2012).

Subtropical SSTs during the early Eocene estimated from TEX_{86} values and isotopic compositions of extraordinarily well-preserved foraminifera around Tanzania (paleolatitude of 19°S) show temperatures greater than 30 °C (Pearson et al., 2001, 2007) (**Figure 3**). Somewhat cooler, but still warmer-than-modern, SST values are reconstructed near the central equatorial Pacific (Huber, 2008; Kozdon et al., 2011; Tripati and Elderfield, 2004; Tripati et al., 2003). Peak tropical ocean temperatures are now considered to have been 5–8 °C warmer than today (Huber, 2008; Pearson et al., 2007). Early Eocene

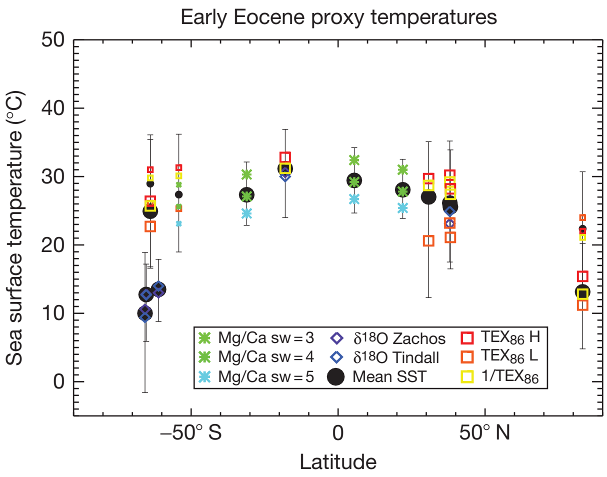

Figure 3 A variety of proxy-based SST estimates for the early Eocene, excluding hyperthermal events. For TEX_{86} reconstructions, several calibrations exist and those are in indicated in the figure legend. Similarly, for Mg/Ca various options exist for the seawater Mg/Ca ratio and those are indicated in the figure legend. Two possible values of the seawater $\delta^{18}O$ are used to estimate the SST from $\delta^{18}O$ values of 'glassy' planktonic foraminifera. The maximum and minimum values of each time series are indicated by the whiskers, whereas the mean value for each proxy record is shown using the colored boxes. Here it is assumed that each estimate is equally likely; for each record, a mean value is calculated and plotted with a black circle. Data are compiled from Lunt et al. (2012).

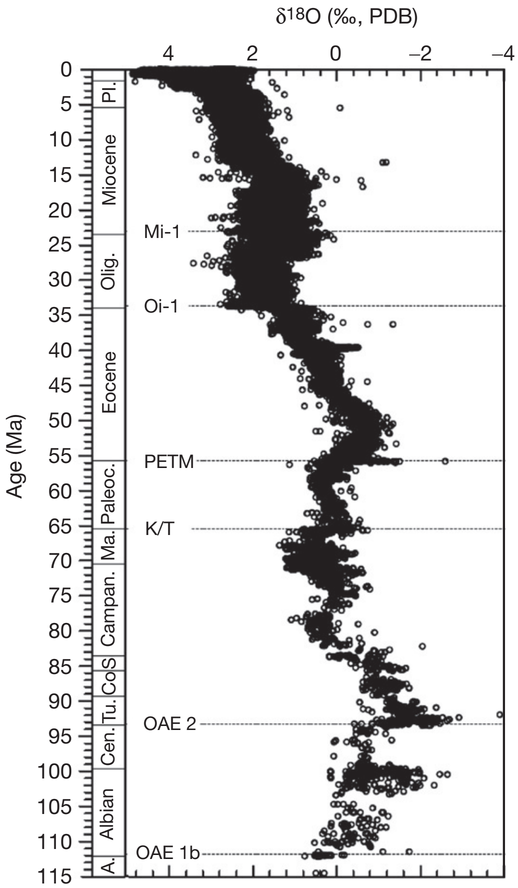

Figure 4 Stable oxygen isotope compilation of benthic foraminifera (modified from Friedrich O, Norris RD, and Erbacher J (2012) Evolution of middle to Late Cretaceous oceans – A 55 m.y. record of Earth's temperature and carbon cycle. *Geology* 40: 107–110 and Cramer BS, Toggweiler JR, Wright JD, Katz ME, and Miller ME (2009) Ocean overturning since the late Cretaceous: Inferences from a new benthic foraminiferal isotope compilation. *Paleoceanography* 24: PA4216). OAE, oceanic anoxic event; K/T, Cretaceous–Tertiary boundary; PETM, Paleocene–Eocene thermal maximum; Oi-1, major Oligocene glaciation; Mi-1, major Miocene glaciation; A, Aptian; Cen, Cenomanian; Tu, Turonian; Co, Coniacian; S, Santonian; Campan, Campanian; Ma, Maastrichtian; Paleoc, Paleocene; Olig, Oligocene; Pl, Pliocene.

mean-annual SSTs at the North Pole are as high as 14 °C (Brinkhuis et al., 2006) to 19 °C (Sluijs et al., 2006) estimated from TEX_{86} values. SSTs approximately as warm as these subtropical values are reconstructed for New Zealand and surrounding regions near 55° S (Bijl et al., 2010; Creech et al., 2010; Hollis et al., 2009, 2012). Antarctic coastal terrestrial temperatures during the early Eocene based on the presence of near-tropical floras suggest MATs of 16 °C, mean winter temperatures of 11 °C, and mean summer temperatures of 21 °C (all with a ±5 °C uncertainty) (Pross et al., 2012). Thus, early Eocene polar annual-mean temperatures were at least 14 °C and perhaps as high as ~30 °C. Existing records from the subtropics to tropics could be interpreted as suggesting peak temperatures of ~35 °C (with a ±5 °C uncertainty) and suggest an early Eocene temperature gradient of somewhere between 20 and 0 °C (**Figure 3**).

Cooling is evident toward the middle and late Eocene (Brinkhuis et al., 2006; Lear et al., 2008; Pross et al., 2012; Zachos et al., 2001), and evidence for the onset of substantial and 'permanent' polar glaciation does not appear until the end of the Eocene/earliest Oligocene ~34 Ma ago (Zachos et al., 1999) (**Figure 4**).

The early Eocene was also a very wet time over much of the world (Sheldon and Retallack, 2004). High latitudes experienced much higher-than-modern precipitation (Greenwood et al., 2010). Fossil leaf characteristics suggest North America maintained much more humid conditions than present (Wilf et al., 1998). Lateritic soil horizons, indicative of warm moist climates, developed up to approximately 45° latitude in both hemispheres (Frakes, 1979), with evidence of paratropical rainforest biomes on the margin of Antarctica suggesting more than a meter of rainfall per year (Pross et al., 2012). The appearance and massive deposition of the fresh-water fern *Azolla*, throughout the Arctic Ocean indicates seasonal or continual persistence of very low-salinity surface waters (Brinkhuis et al., 2006) and implies substantial changes in poleward water-vapor transport during peak temperatures (Pagani et al., 2006b; Speelman et al., 2009, 2010). Nevertheless, even within this broad, very warm interval, compelling evidence supports substantial climate variability and extreme warming events.

6.13.3 The Paleocene–Eocene Thermal Maximum and Other Eocene Hyperthermals

Over and above the extraordinary warmth of the early Eocene are unusually severe and abrupt periods of climate variability, termed hyperthermals (Lourens et al., 2005; Thomas and Zachos, 2000; Zachos et al., 2001). To date, three major hyperthermals have been identified: the Paleocene–Eocene

Figure 5 The sedimentary expression of hyperthermal events in the Scaglia Rossa Formation of the Possagno outcrop (Southern Alps, Veneto, Italy). Hyperthermals correspond to marly interval intercalated in the red limestone succession due to carbonate dissolution and increased terrigenous input. Cyclical marly layers in the upper part of the stratigraphic succession corresponds to the Early Eocene Climatic Optimum interval. The section is described in Agnini et al. (2006). Image from Luca Giusberti and Domenico Rio.

Thermal Maximum (referred to as the PETM or Eocene Thermal Maximum 1), Eocene Thermal Maximum (ETM) 2 (also referred to as ELMO), and ETM3 (also referred to as the X-event) (**Figure 5**). During the PETM at ~55 Ma, temperatures are reconstructed to have increased by 5–8 °C in southern high-latitude sea-surface waters (Kennett and Stott, 1990), about 4–5 °C in the Arctic Ocean (Sluijs et al., 2006) and equatorial surface waters (Kozdon et al., 2011; Zachos et al., 2005), and the deep sea (Zachos et al., 2001). Warming was also about 5 °C at middle latitudes in continental interiors (Fricke and Wing, 2004; Wing et al., 2005) and along the Arctic coast (Weijers et al., 2007). Diversity and distribution of marine biota (Bralower, 2002; Kelly et al., 2001; Speijer and Morsi, 2002) and terrestrial flora shifted (Wing et al., 2005), with migration of thermophilic biota to high latitudes and evolutionary turnover (e.g., Gingerich et al., 1980; Hooker, 1996; Maas et al., 1995). Deep-sea benthic foraminifera suffered extinction of 30–50% of species (Kennett and Stott, 1991, 1995; Thomas, 2007; Thomas and Shackleton, 1996).

The PETM is also associated with a severe shoaling of the ocean calcite compensation depth and a ≥3.0‰ negative stable carbon isotope excursion (CIE) reflected in marine and soil carbonates. The confluence of ocean acidification, the CIE, and temperature proxy records, leads to the conclusion that the PETM and other hyperthermals represent a massive release of ^{13}C-depleted carbon and CO_2-induced global warming.

It appears that each hyperthermal exhibits many of the same characteristics including a transient warming, a stable carbon isotope excursion, benthic foraminiferal assemblage changes, and dissolution horizons (Lourens et al., 2005; Zachos et al., 2005). However, the magnitude of the CIE for each subsequent warming event decreases (Sluijs et al., 2009; Stap et al., 2010). Hyperthermals also appear to correspond to similar combinations of orbital parameters (DeConto et al., 2012; Galeotti et al., 2010; Lourens et al., 2005) and support the notion that hyperthermals were driven by a common trigger. If Paleocene climate sensitivity was in the probable range of 'fast feedback' climate sensitivities for modern conditions (e.g., 2–4.5 °C per doubling of CO_2), the implied carbon dioxide release for the PETM and other hyperthermals was massive in order to cause the observed temperature changes in a world that already had high concentrations of greenhouse gases. Alternatively, climate sensitivity during the early Eocene was higher than average values estimated for today, perhaps because more feedbacks were allowed to come into play (known as Earth System climate sensitivity) given the large magnitude of forcing and the duration over which climate change occurred (Dickens et al., 1995; Higgins and Schrag, 2006; Pagani et al., 2006b; Zeebe et al., 2009).

The source of carbon to cause these hyperthermals is theoretically constrained by the size of the CIE, the carbon isotope composition of the source carbon, and changes in the carbonate compensation depth determined by the degree of carbonate dissolution (Jones et al., 2010; Panchuk et al., 2008; Zeebe et al., 2009). Two dominant hypotheses for extreme warming have emerged with distinctly different implications for the climate system during greenhouse climates. A common explanation invokes a massive release of methane gas precariously trapped in marine sediments as methane clathrates (Dickens et al., 1995). In this scenario, clathrates are destabilized and methane is either oxidized in the water column and/or released to the atmosphere where it is quickly converted to CO_2. The methane hypothesis requires the initial release of ~3000 PgC during the PETM (Zeebe et al., 2009) driven by a rapid pre-event warming and/or threshold temperatures in very deep waters given that methane clathrates would only be stable in deep pelagic sediments where high sedimentary pressures offset the enhanced warmth of the Eocene deep ocean (Archer and Buffett, 2005; Archer et al., 2004). The cause and nature of this 'pre-event warming' has not been defined or well identified in paleotemperature reconstructions (Sluijs et al., 2007), and is further constrained by the appearance of orbital controls on the occurrence of hyperthermals. Whether or not the necessary quantity of methane was even available during greenhouse times is another important debate (Archer et al., 2004; Buffett and Archer, 2004; Dickens, 2011). If methane was indeed the primary source of carbon responsible for extreme warming, it suggests that Earth System climate sensitivity to CO_2 (i.e., climate sensitivity that includes slow and fast feedbacks) was high during the Eocene given the estimates of carbon released (Higgins and Schrag, 2006; Pagani et al., 2006b; Zeebe et al., 2009), even though cryospheric effects were absent.

An alternate hypothesis for the appearance of hyperthermals calls on the irreversible degradation of biomass (DeConto et al., 2012; Higgins and Schrag, 2006; Kurtz et al., 2003) leading to direct release of CO_2 into the atmosphere. This has been proposed to occur as tropical ecosystems crossed thermal thresholds (Huber, 2008) or as high-latitude permafrosts warmed, dried, and subsequently experienced oxidation of accumulated soil organic carbon (DeConto et al., 2012). However, the apparent coincidence of hyperthermals with combined high eccentricity and high obliquity (Lourens et al., 2005) implicates changes in high-latitude seasonal insolation as the ultimate trigger (DeConto et al., 2012). In this scenario, high-latitude permafrost catastrophically melted when the region crossed a critical temperature threshold due to the combination of slow, CO_2-induced warming and warm orbital geometries. CO_2 is then released from the oxidization of permafrost organic carbon. The upper range of model-derived estimates for the amount of available permafrost carbon (DeConto et al., 2012), as well as modern rates of permafrost carbon sequestration and release (Schuur et al., 2008, 2009), accommodate geochemical requirements dictated by carbon cycle modeling (Cui et al., 2011; Panchuk et al., 2008) and lead to much higher CO_2 input and lower estimates of Earth System climate sensitivity (Jones et al., 2010; Pagani et al., 2006b). However, the requirement that permafrost existed on Antarctica during the early Eocene might be hard to reconcile with recent evidence for pervasive Antarctic coastal warmth during the interval (Hollis et al., 2012; Pross et al., 2012).

Presently, carbon cycle models do not allow us to discriminate between various carbon cycle perturbation hypotheses. In lieu of novel results from new geochemical proxies, determining which of these hypotheses represent the primary hyperthermal trigger will depend on an improved understanding of how ocean pH changed and impacted the global CCD, as well as a clearer understanding of the limits of methane and terrestrial carbon reservoir magnitudes and accumulation rates during a much warmer world. Nonetheless, these hypotheses suggest that extreme climate variability is an aspect of greenhouse climates particularly as the climate system evolves from the colder spectrum of the greenhouse world toward the warmest extremes and threshold conditions.

6.13.4 The Case For and Against Glaciations During Greenhouse Climates

In spite of profound global and high-latitude warmth during the most recent greenhouse episode, arguments persist for icehouse conditions or punctuated glaciations during the Cretaceous (Bornemann et al., 2008; Miller, 2009; Price and Nunn, 2010; Steuber et al., 2005) and the Eocene (Spielhagen and Tripati, 2009), challenging the notion of a strictly ice-free planet during prevalent greenhouse conditions (Frakes and Francis, 1988). Intriguing evidence for seasonally freezing temperatures and/or permanent polar ice includes ice-rafted debris and lonestone-bearing mudstones together with glendonite pseudomorphs on Australia during the early Cretaceous Valanginian through the Albian stages (Alley and Frakes, 2003; Frakes et al., 1995; Price, 1999; Price and Nunn, 2010). Deposits with glendonites, single erratics, and conglomeratic clasts have also been found in Paleocene–Eocene sections on Svalbard (Spielhagen and Tripati, 2009). Of these deposits, a distinct 2-m thick Cretaceous diamictite on Flinders Range of Australia represents evidence for glacial erosion (Alley and Frakes, 2003). Although these observations are supportive of cool, higher latitude/altitude temperatures, they are not considered unambiguous evidence of continental ice sheets (Bennett and Doyle, 1996; Hay, 2008). Single erratics and clasts can often be discounted as anomalous dispersal by kelp or storm deposits (as discussed in Markwick, 1998), but glendonite pseudomorphs are more difficult to discount.

Three interpretations of these sedimentological records can be made. First, the appearance of high-latitude warmth from nearly all the other proxies is incorrect and these climates were actually perennially cooler than most reconstructions. While this would certainly reduce the model-data discrepancies that have pervaded the literature, the overwhelming bulk of proxy evidence leads us to conclude that this argument is not valid. The second alternative is that these are records of short, 'cold snaps' (Price and Nunn, 2010) probably related to orbital configurations that enhance polar cooling. Whether this hypothesis is valid is debatable (Jenkyns et al., 2012), but the argument is physically plausible. A third alternative is that records of cool high-latitude temperatures – the presence of glendonite pseudomorphs formed after ikaite – represent filters of the seasonal variability that are especially sensitive to winter season temperatures. For example, the presence of ikaite tends to be interpreted as indicating subseafloor temperatures of <4 °C (Spielhagen and Tripati, 2009) or <7 °C (Price and Nunn, 2010), both of which are compatible with the densest water temperatures that might occur in the winter season in the Arctic while still being consistent with other proxy records. In other words, the presence of cold sensitive proxies such as pseudomorphs could simply be revealing colder winter season temperatures (4–7 °C) preferentially recorded in the densest waters at depth in enclosed basins.

Interpretations of sea-level variations during the Cretaceous and Eocene present an additional challenge to the assumption of ice-free conditions. Recent reviews by Hay (2008) and Miller et al. (2011) provide a comprehensive summary of the greenhouse glacioeustasy debate. Evidence for glaciation rests mainly on inferred eustatic fluctuations from stratigraphic sequences occurring at frequencies too high for tectonic drivers. Some of these sequences are also argued to be linked to stable isotope variability and astronomical pacing (e.g., Boulila et al., 2012; Gale et al., 2008; Galeotti et al., 2009). Accordingly, opposition to greenhouse glacioeustasy falls into two broad camps: those who question eustatic reconstructions based on ancient stratigraphic successions (e.g., Burton et al., 1987; Fjeldskaar, 1989; Miall, 1992; Morner, 1976) and those who argue that isotopic data do not support changes in ice volume large enough to account for glaciation (Ando et al., 2009; Moriya et al., 2007). Initial estimates of eustatic sea-level- and inferred ice-volume changes from stratigraphic sequences (Haq et al., 1987; Vail et al., 1977) failed to adequately consider the potential for isostatic adjustments, changes in sediment load, dynamic topography associated with the viscous flow response of the mantle (Lambeck and Chappell, 2001; Mitrovica et al., 2011), basin subsidence (Christie-Blick et al., 1990; Hay, 2008; Hay and Southam, 1977), and autocyclic depositional processes such as delta migration and progradation (e.g., Poulsen et al., 1998). As a consequence, those sea-level estimates appear unreasonably large, requiring volumes of ice equal to or greater than the current Antarctic ice sheet to wax and wane during extraordinarily warm periods (e.g., Hay, 2008).

More recent sea-level reconstructions (**Figure 6**) that employ corrections for isostacy, sediment loading, and subsidence (e.g., Kominz et al., 2008; Miller et al., 2005a) limit oscillations prior to the Neogene expansion of ice sheets to a maximum of about 50 m – which would still require significant ice volumes if glacioeustasy was the only driver. Although there is a reasonable match between the long-term pattern in $\delta^{18}O$ (and by inference temperature) and the long-term sea-level record (**Figure 6**), the attribution of high-frequency

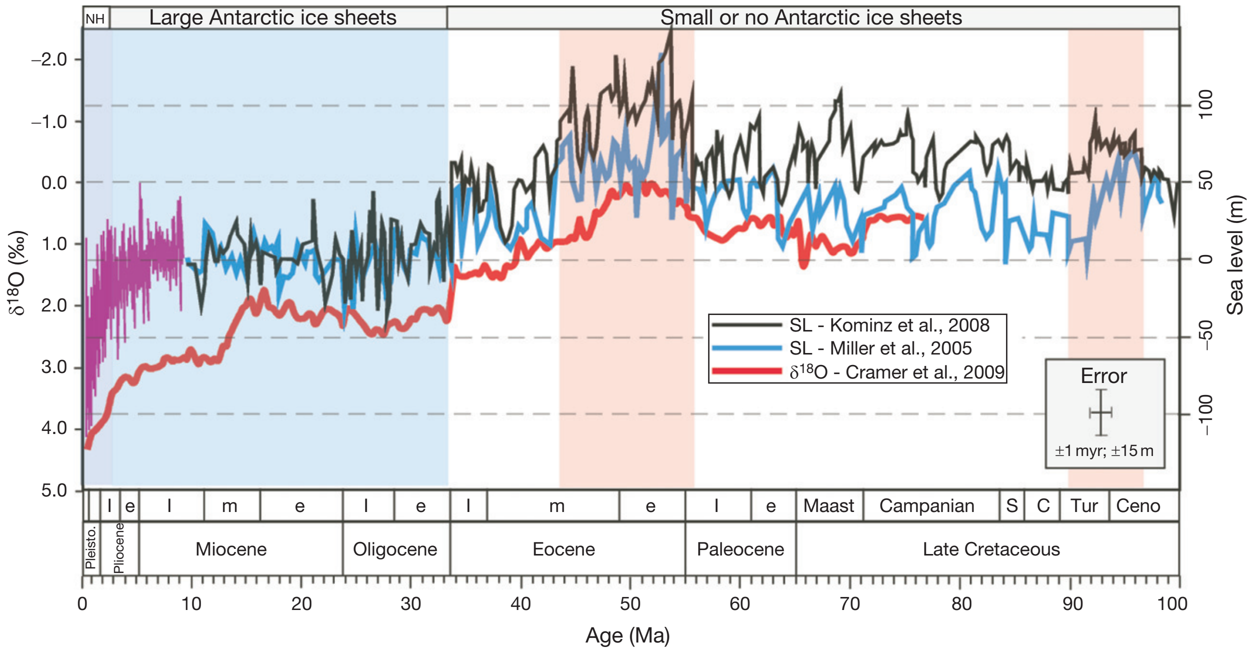

Figure 6 A reconstruction of sea level complied by Miller et al (2011) is based on integration of stratigraphic, geochemical, and paleontologic data from the New Jersey continental margin (Kominz et al., 2008; Miller et al., 2005a) and incorporates corrections for compaction, loading, and thermal subsidence. Also shown are oxygen isotope data of Cramer et al. (2009). The two bands of reddish color mark Cretaceous and Eocene 'hyperthermal' intervals characterized by elevated sea levels, and the blue and darker blue bands mark development of Antarctic and Northern Hemisphere continental ice sheets, respectively, characterized by the lowest sea-level stands of the last 100 Ma. NH, Northern hemisphere ice sheets.

oscillations from one region to a glacioeustatic mechanism faces a significant challenge. The chronostratigraphic resolution of Mesozoic and Cenozoic successions has progressively increased (e.g., Kuiper et al., 2008; Meyers et al., 2012), but the potential for error associated with global stratigraphic correlations make most chronostratigraphic frameworks insufficient to conclusively prove or disprove the global synchroneity of events that are within very narrow (orbital) time scales (e.g., Raymo et al., 2011). As continental ice is loaded and unloaded across high-frequency Milankovitch periodicities, high-resolution correlation of distal stratigraphic sequences do not necessarily provide comparable interpretations of eustasy given that regional stratigraphic records could capture variable magnitudes, timings, and/or direction (rise or fall) of sea-level change (Mitrovica et al., 2001, 2011; Raymo et al., 2011). On the other hand, predicted variations to ice-volume change on Antarctica only (e.g., Mitrovica et al., 2011) show that it is possible for sites in different parts of the Northern Hemisphere (where most Cretaceous high-resolution stratigraphic work has been focused) to record coherent eustatic responses. Further, longer period orbital cycles (1.2 Ma obliquity; 400 ky and 2.4 Ma eccentricity) have been receiving increasing attention because they involve larger amplitude changes and are more likely to average out regional variations in the eustatic signal (Boulila et al., 2012).

Another line of evidence for greenhouse glacioeustasy, the correlation of geochemical ice volume proxies to sea-level records (e.g., Boulila et al., 2012), has been challenged by problems stemming from diagenetic alteration of carbonate minerals. For example, changes in the strontium content of carbonates with assumed correspondences to eustatic sea-level changes during the Early Cretaceous have been interpreted as reflecting shifts in the Sr content of the ocean related to the alteration of Sr-rich aragonitic carbonates as sea-level fell and rose over 200–500 kyr timescales (Stoll and Schrag, 1996). Less convincingly, bulk $\delta^{18}O$ records from central Italy are argued to support the growth of mid-Cretaceous ice and resulting large-scale sea-level variations (Stoll and Schrag, 2000). A major criticism of $\delta^{18}O$ and Sr/Ca data from bulk carbonates of adjacent calcareous shales/marlstones and limestones is susceptibility to diagenetic processes (associated with compaction and pressure solution) that transfer carbonate from $CaCO_3$-poor to $CaCO_3$-rich beds, enriching the higher carbonate end member with cements depleted in Sr and ^{18}O, with an end result that appears to favor a glacioeustatic interpretation (Frank et al., 1999). Extensive efforts have been made to isolate unaltered calcite for analysis (Ando et al., 2009; Huber et al., 2002; Moriya et al., 2007) and although these studies conclude that the data do not support an interpretation of major ice-volume changes, others interpret the same data differently (Miller et al., 2011).

High-resolution isotopic trends from extremely well-preserved surface-dwelling and benthic foraminifera from the same site on Demerara Rise (Moriya et al., 2007) and less well-preserved foraminifera from Blake Nose in the subtropics of the North Atlantic (Ando et al., 2009), fail to detect co-variance in low-latitude, shallow- and deep-dwelling isotopic compositions, as would potentially occur during large-scale continental glaciations. On the other hand, variations in vertical ocean density gradients due to climate change might obscure such relationships. Key unknowns include ice-mass changes (because there may be synchronous and complimentary sea-level change mechanisms that reduce the amount of ice needed for a given eustatic oscillation, and thus smaller isotopic effects), as well as assumptions about the isotopic composition of Cretaceous ocean water and precipitation, which influence the proxy relationship.

The most convincing records of large magnitude sea-level changes are high-frequency, inferred eustatic oscillations observed during the Early- to Late Cretaceous, including some during the peak warming of the Middle Cretaceous from the Western Interior North America (Gale et al., 2008; Koch and Brenner, 2009), Europe, India (Gale et al., 2002), and central Italy (Galeotti et al., 2010, Weissert and Lini, 1991). Putatively, eustatic sea-level estimates from New Jersey, USA and the Russian platform for the Late Cretaceous to early Eocene (including some for the Middle Cretaceous), which are assumed correlative with positive changes in low-resolution benthic $\delta^{18}O$ values from other locations (Huber et al., 1999, 2002), are interpreted as ~25 m of sea-level change occurring in less than 1 Ma (Miller et al., 2005a,b; Sickel et al., 2004).

Other perspectives that support the notion of greenhouse glaciation apply TEX_{86} temperatures in conjunction with well-preserved foraminiferal oxygen isotopes from the Demerara Rise in the eastern equatorial Atlantic (Bornemann et al., 2008; Forster et al., 2007a,b). Large changes in ice volume – from ~45 to 150% the size of the modern Antarctic ice sheet – are calculated during peak temperatures in the Turonian on the basis of positive $\delta^{18}O$ shifts that are unmatched by TEX_{86} changes. Even though the baseline tropical temperatures estimated by the same study are ~10 °C warmer than today (i.e., 34–37 °C) (Bornemann et al., 2008), the authors settle on ice volumes perhaps 60% the size of the modern Antarctic ice sheet, given other constraints from stratigraphically inferred sea-level changes. However, how ice sheets of this magnitude can move on and off under apparent 'supergreenhouse' conditions with less than 2 °C of tropical temperature change (as indicated by TEX_{86} temperatures) is not addressed.

The accuracy of TEX_{86} temperatures is a subject of increasing debate. Much of the current discussion is focused on the depth of production and the ocean temperatures that the TEX_{86} proxy actually reflects (e.g., Ingalls et al., 2006; Liu et al., 2009; Shah et al., 2008). Given the potential of ammonia oxidation by nonthermophilic Thaumarchaeota (e.g., Nicol and Schleper, 2006), depth of production over time and space can be unconstrained, and so the interpretation that TEX_{86} exclusively reflects SST is not necessarily warranted. It also remains to be seen if TEX_{86} values are solely recording temperature. For example, other organic-based temperature proxies, such as $U_{37}^{K'}$ values and alkenone abundances are affected by species composition (Conte et al., 1998), salinity (Blanz et al., 2005), and levels of nutrients and irradiance (Prahl et al., 2003). Turich et al. (2007) challenges a strict SST interpretation for TEX_{86} and argues that nutrient distributions and ecology of Archaea play roles in the distribution of membrane lipids and the expression of residual temperature offsets between proxy estimates and modern observations. To date, there is no overwhelming challenge to the accuracy of TEX_{86} SST temperatures other than the persistence of multiple calibrations that result in a broad range of temperature estimates (Kim et al., 2010; Liu et al., 2009), and the occasional observation that the estimated temperatures reflect deeper water production rather than SST (e.g., Liu et al., 2009). Still, a healthy concern for the accuracy of absolute values of TEX_{86} temperatures, particularly across the high latitudes during greenhouse climates is warranted given the sometimes stark differences between TEX_{86} and other proxy results (Liu et al., 2009).

If other mechanisms used to explain apparent greenhouse eustatic oscillations, such as thermal expansion/contraction and changes in groundwater storage in response to climate forcing – with the potential of up to ~10 m of sea-level change (Hay, 2008) – were operative on orbital time scales, the volume of ice build-up might be modest enough to preclude large oxygen isotopic signals (Miller, 2009). The location of significant ice accumulation during Cretaceous and Cenozoic greenhouse times is necessarily restricted to Antarctica (Hay, 2008), and modeling studies have shown that it is possible to grow ice sheets under conditions of elevated CO_2 (DeConto and Pollard, 2003; Flögel et al., 2011). Removal of a substantial ice sheet, however, requires either very large increases in CO_2 due to hysteresis in the Antarctic ice sheet – implying wild swings in atmospheric CO_2 concentration (Pollard and DeConto, 2005) – or significant changes in insolation related to linkage of long period astronomical cycles and their amplification by feedbacks such as the carbon cycle (e.g., Boulila et al., 2012; Pälike et al., 2006).

Direct evidence of Antarctic glaciation in the Cretaceous has yet to be revealed and would provide the most unambiguous indication of significant ice volume during extraordinary warmth. As such, the hypothesis that greenhouse sea-level oscillations were modulated by orbitally paced climatic cycles, that also involved global 'cold snaps' during some of the warmest intervals of Earth history, has yet to be conclusively demonstrated.

6.13.5 Greenhouse Climates and Organic Carbon Burial

The association of widespread black shale facies with greenhouse climates or 'nonglacial' periods was recognized early on (Chamberlin, 1906; StrØm, 1936; van der Gracht, 1931), as was a correlation between organic matter enrichment and distal sediment starvation during marine transgressions (e.g., Pettijohn, 1957). A series of papers in the 1970–1980s synthesized these and other ideas into a coherent framework of greenhouse/icehouse oscillations mediated by changes in global volcanism, CO_2 levels, surface- and deep-ocean temperatures, flooding of continental interiors, and changes in the occurrence of black shale deposition (e.g., Fischer, 1982; Fischer and Arthur, 1977). Two major greenhouse climate intervals during the Paleozoic and Mesozoic are characterized by widespread black shale facies, and particular attention has been paid to the relationships between warm climates and black shale deposition during the Devonian and Cretaceous.

Characteristics most relevant among Cretaceous black shales are stratigraphically narrow, but widespread horizons of exceptional organic carbon deposition that punctuate sedimentary successions (e.g., Erbacher et al., 2005). These global carbon cycle perturbations, known as 'Oceanic Anoxic Events' (OAEs) (Schlanger and Jenkyns, 1976) are associated with significant positive shifts in the stable carbon isotope signature of organic and inorganic carbon (Arthur et al., 1988; Pratt, 1985). OAEs are interpreted to reflect substantial marine

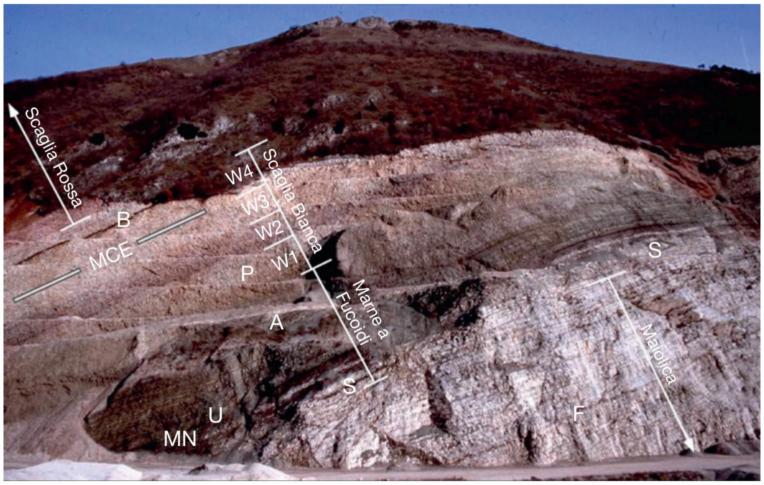

Figure 7 The Vispi Quarry in the Contessa Valley, near Gubbio, Italy – the most spectacular outcrop of pelagic Cretaceous sediments in the Umbria-Marche Basin. The most prominent organic-rich horizons include: F = Faraoni Level (uppermost Hauterivian); S = Selli Level (OAE 1a, early Aptian); MN = Monte Nerone Level and U = Urbino Level (OAE 1b, early Albian); A = Amadeus Segment (OAE 1c, late Albian); P = Pialli Level (OAE 1d, latest Albian); B = Bonarelli Level (OAE 2, latest Cenomanian). W1, W2, W3, W4 are the members of the Scaglia Bianca Formation (image from Coccioni and Galeotti, 2003).

organic-carbon burial and bottom-water anoxia, and in some cases, contributed to biological extinctions. It is also hypothesized that carbon burial during some OAEs helped drawdown atmospheric carbon dioxide and impact the character of the greenhouse climate (Arthur et al., 1988; Barclay et al., 2010) (**Figure 7**). Although there are geochemical and stratigraphic differences among formally recognized OAEs, at least two Cretaceous events, the Selli (late early Aptian; ~120 Ma) and Bonarelli (Cenomanian–Turonian; ~93.5 Ma), are expressed globally and indicative of ocean-wide anoxia at least at intermediate water depths (Leckie et al., 2002). During these OAEs, oxygen isotopic- and TEX_{86} records suggest extremely warm global temperatures, with equatorial SSTs of 32–36 °C and polar temperatures in excess of 20 °C (e.g., Forster et al., 2007a,b; Huber et al., 2002; Norris et al., 2002).

The number and diversity of hypotheses proposed to explain OAEs reflect both the complexity of these geological phenomena and the limitations of our understanding. The most credible suppositions for the two large-scale OAEs relate to major changes in ocean circulation associated with the opening of oceanic gateways (Poulsen et al., 2001) and the impact of massive volcanism on ocean chemistry and atmospheric composition (Kerr, 2005).

Sluggish thermohaline circulation, due to low meridional-temperature gradients (e.g., Demaison and Moore, 1980), was long hypothesized as an important characteristic of greenhouse climates, but is not consistent with recent modeling that requires an overturning ocean to produce the massive production of organic carbon buried during OAEs (Meyer and Kump, 2008; Poulsen et al., 2001). Accordingly, opposing arguments requiring active ocean circulation during the Late Cretaceous have recently been proposed (Alexandre et al., 2010; Hay, 2008; Poulsen et al., 2003), an interpretation more consistent with the necessity of enhanced surface-water nutrient flux during Cretaceous OAEs (Adams et al., 2010; Mort et al., 2007).

The role of volcanism has received increasing attention in recent years, in part because of new geochemical evidence in support of it. An increase in volcanic and hydrothermal activity, perhaps associated with Large Igneous Provinces (LIPs), which increased atmospheric pCO_2 and temperature, enhanced weathering rates, increased nutrient fluxes to the oceans, and altered ocean chemistry, which substantially enhanced ocean export productivity (e.g., Adams et al., 2010; Frijia and Parente, 2008; Kerr, 1998; Kuroda et al., 2007; Sinton and Duncan, 1997; Turgeon and Creaser, 2008).

The emplacement of LIPs was sporadic and rapid on geological timescales, but produced almost three times as much oceanic crust in the Cretaceous (considering LIPs and spreading centers) as in any comparable period (e.g., Larson 1991a, b). As a consequence, fluxes of greenhouse gases and other chemical constituents, including nutrients, appear unusually large compared to the remainder of the sedimentary record. The direct impact of LIP volcanism on large-scale circulation through changes in the geothermal heat flux was probably small, but perturbations to circulation within isolated abyssal basins might have been important. Similar processes can be invoked for Paleozoic black shales, especially those marked by significant carbon isotope excursions like during the Late Devonian Kellwasser events (Joachimski and Buggisch, 1993), but the lack of preserved ocean crust and pelagic sediments during these more ancient times makes it difficult to substantiate ocean-wide anoxia. Although the Eocene is not devoid of black shales (e.g., Al-Hajari and Khaled, 1994) and includes interesting examples of 'fresh-water' organic-rich deposits in the Arctic (Boucsein and Stein, 2009; Brinkhuis et al., 2006), the stratigraphic extent and geographic distribution of marine black shales in the Eocene is far less than that of Mesozoic and Paleozoic greenhouse intervals. Organic carbon burial in the semi-enclosed Tethys Ocean could have played an important role in the recovery from the Middle Eocene Climatic optimum (Spofforth et al., 2010), but generally speaking, organic carbon burial rates in the major ocean basin (the Pacific Ocean) were anomalously low (Olivarez Lyle and Lyle, 2006). In this regard, there appears to be a fundamental difference between the greenhouse climates of the Cenozoic and Mesozoic/Paleozoic, perhaps indicating that greenhouse climates are a necessary, but not sufficient condition for widespread black shale deposition and OAE development. The character of OAEs demands episodic disruptions and substantial nutrient fluxes to sustain the widespread distribution of organic-rich black shales. Other mechanisms were likely in play and major changes in ocean circulation related to plate tectonics could have played a key role (Robinson and Vance, 2012).

6.13.6 Climate Modeling and the Challenges of Greenhouse Temperature Distributions

Whereas modern discussions of climate change dwell in the minutia of exceedingly short time scales and global temperature variations within tenths of a degree, greenhouse intervals provide a means to test fundamental assumptions regarding the first-order controls on Earth's temperature, as well as the strengths/weaknesses of our current climate models under large climate changes. The primary factors driving regional temperature distributions, and in particular, global mean temperature and latitudinal temperature gradients, have been explored through the course of climate modeling history.

6.13.6.1 The Low Temperature Gradient Problem in a Warmer World

Initial efforts to model Cretaceous greenhouse climates focused on paleogeography and its role in altering planetary albedo. The earliest paleoclimate modeling experiments using simple albedo calculations (Barron et al., 1980) and a planetary albedo model (Thompson and Barron, 1981) indicated an important role for paleogeography and land–sea distributions in altering Earth's radiative balance, accounting for a 2.3% increase in absorbed insolation during the Cretaceous and an approximate 2 °C change in global mean temperatures. A more advanced atmospheric circulation model (Barron et al., 1981) expressed a slightly lower global temperature gain of 1.6 °C (largely occurring because of a polar temperature increase of 5 °C) solely by paleogeographical reconstructions and an assumption of ice-free conditions. An additional degree of global temperature increase resulted by ascribing a broad distribution of lush terrestrial vegetation. A first-generation general atmospheric circulation model (GCM) also implied that paleogeography influenced aspects of large-scale atmospheric circulation (Barron and Washington, 1982). Together, simulated paleogeography and vegetation accounted for ~30% of the temperature increase relative to today observed as reconstructed for the Cretaceous from publications in the 1980s (note: since newer reconstructions are warmer, a smaller component of the temperature change between the Cretaceous and today can be accounted for by such boundary condition changes). Simulated polar temperatures remained below freezing and meridional gradients were much higher than proxy reconstructions. Ad hoc manipulations, such as a reduction in the vertical atmospheric temperature gradient, and a more uniform and lower average cloud coverage, helped reduce meridional-temperature gradients, but did not remotely approach observations.

The next generation of simulations using a GCM coupled to a simple 'swamp' ocean with more realistic topographic and land–sea reconstructions, a more advanced cloud parameterization, and an improved hydrologic cycle provided continued support for a more substantial, first-order temperature effect related to paleogeography (4.8 °C increase in mean temperatures relative to Modern conditions) (Barron and Washington, 1984). More recent experiments continue to suggest an important role for paleogeography in increasing global temperatures and reducing meridional-temperature gradients by attenuating seasonality through an increase in latent-heat transport to continental interiors, leading to a wetter and a cloudier winter (Donnadieu et al., 2006). However, results were still far from satisfying the temperature differences between the Cretaceous and present climates.

Two dominant observations emerged from the initial, as well as more advanced modeling attempts: (1) low meridional-temperature gradients (**Figure 8**) are difficult to explain, and (2) changes in albedo, paleogeography, and solar flux cannot account for the warmth of the greenhouse Earth. Climate models have historically failed to reproduce the small equator-to-pole temperature gradients indicated by paleoclimate data

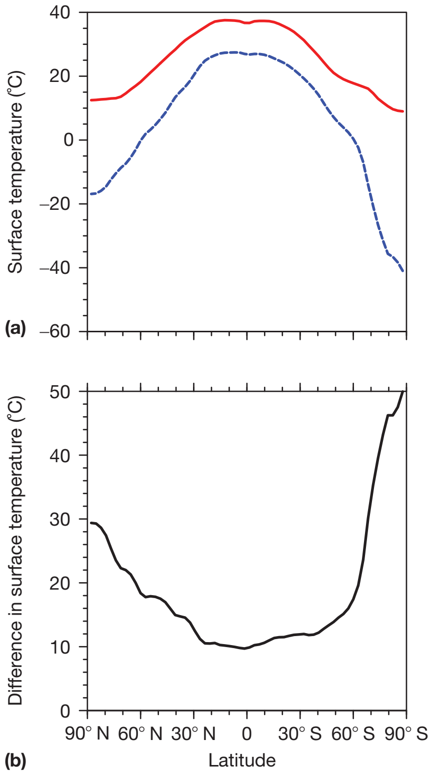

Figure 8 (a) Zonal mean surface temperature from the Eocene climate model simulations carried out at 4480 ppm CO_2 (red) and modern simulated temperatures (blue). The modern and Eocene-simulated temperatures are very close to observations and proxy reconstructions as described in Huber and Caballero (2011). (b) The zonal mean surface temperature anomaly demonstrating the marked decrease in meridional-temperature gradient reproduced in the Eocene simulation.

(Barron, 1987; Deconto et al., 2000; Huber and Sloan 2000, 2001; Sloan and Rea, 1996; Valdes, 2000), a problem exacerbated by recent proxy temperature estimates that have raised polar temperatures more than those in the tropics.

6.13.6.2 The Role of Ocean Heat Transport

Increased poleward heat transport by the ocean or atmosphere has long been considered a solution to the low-gradient problem (Berry, 1922; Barron, 1987; Barron et al., 1993; Covey and Barron, 1988; Rind and Chandler, 1991; Schmidt and Mysak, 1996). However, the supposition of low gradients propelled by enhanced heat transport is recognized as a climate conundrum: that is, enhanced ocean heat transport is necessary to maintain low meridional-temperature gradients, but small meridional-temperature gradients imply reduced density gradients, decreased meridional overturning circulation, and hence reduce rates of poleward heat transport. For Cretaceous and Eocene experiments, total ocean heat transport greater than modern values have often been necessary to avoid overly high tropical- or cold polar temperatures (Barron et al., 1981; Huber and Sloan, 1999). Given the physical constraints on the atmosphere's ability to transport more heat under equable conditions, other mechanisms, including ocean heat transfer in the form of low-latitude halothermal circulation, were hypothesized. Justifications for enhanced ocean heat transport reach back to Chamberlin (1906) who called on the production of high-salinity waters sourced from highly evaporative, low-latitude regions during warm periods in Earth history. But, arguments regarding the source of deep waters and the direction of transport miss the mark (Bice and Marotzke, 2001). The magnitude of ocean heat transport due to advective motions is determined by the amount of cooling and the vigor of ocean circulation. It is the heat released to the atmosphere that is relevant and this is recorded by the cooling of watermasses as they move poleward. Weak temperature gradients imply weak ocean heat transport regardless of whether deep water forms at high latitudes or low latitudes (Huber et al., 2003). Thus, production of 'warm saline bottom waters' does not directly solve the major problems of greenhouse climates.

Models that simultaneously predict the behavior of the atmosphere and ocean have only produced total meridional atmospheric and ocean heat transports close to modern (Huber and Sloan, 2001; Lunt et al., 2012; Najjar et al., 2002; Otto-Bliesner et al., 2002; Sijp et al., 2011; Winguth et al., 2010; Zhang et al., 2011), whereas the missing heat transport necessary to simulate greenhouse temperature gradients of 15 °C is inferred to be an extraordinary $\geq$1 Petawatt at 45° latitude (Huber and Sloan, 1999; Huber et al., 2003) – three times the modern value. To achieve this kind of trebling of ocean heat transport in a world with temperature (and thus density) gradients less than half of modern values, requires a greater than sixfold increase in the strength of the meridional overturning circulation. Well-established physical mechanisms cannot provide for this kind of increase, although the idea that vertical diffusion was much stronger in the past and that this enhanced the ocean circulation has been explored in simple models (Emanuel, 2002; Lyle, 1997). There is no evidence from ocean circulation proxies for such large increases in ocean circulation rates (Hague et al., 2012; Pucéat et al., 2007) and the associated decrease in ocean residence time it implies, but such evidence would be very informative.

Importantly, high polar temperatures and low meridional-temperature gradients do not necessarily imply the need for an increase in ocean heat transport relative to modern values if temperature gradients are at the higher end of possible values. For example, an equator-to-pole SST difference of 24 °C (compared to ~50 °C today) requires near-modern heat-transport values, whereas a gradient of 15 °C requires an ocean heat transport three times the modern value (Huber et al., 2003). Reconstructed polar temperatures of 25 °C in conjunction with tropical temperatures of 31 °C would require conditions that strongly deviate from the modern dynamical paradigm, whereas polar temperatures of 15 °C and tropical values of 35° might not. Presently, it is impossible to definitively conclude whether or not we are missing a critical piece of the puzzle in our understanding of ocean heat transport and weak temperature gradients.

6.13.6.3 The Role of Atmospheric Heat Transport

It is often assumed that increased latent-heat transport could account for low, meridional-temperature gradients during greenhouse climates (e.g., Ufnar et al., 2004). However, this conjecture is not as straightforward as it appears. Current theory and models have shown that latent-heat transport increases with an increasing meridional-temperature gradient for a range of global mean temperatures – the opposite to what is required to maintain low temperature gradients (Pierrehumbert, 2002). But, this is complicated by nonlinearity effects introduced by atmospheric moisture. The exponential dependence of atmospheric saturation vapor pressure from the Clausius–Clapeyron relation – which provides an ~7% increase in atmospheric water-vapor content per degree (°C) of global-mean temperature increase (Held and Soden, 2006) – suggests that during greenhouse conditions it is possible to have higher latent-heat transport even with weaker surface temperature gradients because there is more water vapor to transport (Caballero and Langen, 2005; Frierson et al., 2007). The result of Caballero and Langen (2005) show that poleward atmospheric latent-heat transport increases with both increasing temperature gradient and increasing global-mean surface temperature, but global mean temperature would have to substantially increase above modern conditions before this new regime is encountered. Model predictions for latent-heat transport are very sensitive to tropical temperatures because tropical temperatures dominate the uncertainty of area-weighted global mean temperature estimates (the region between 30°N and 30°S makes up half the Earth's surface area). Uncertainties in high-latitude temperatures dominate the uncertainties in a model's expression of the temperature gradient. Models show that the atmosphere can transport more heat relative to modern conditions even with weaker temperature gradients, but only if global mean temperatures are much higher than the modern mean. Whether or not models are producing accurate results is not currently verifiable from proxy data because uncertainty in both tropical- and high-latitude temperatures is large enough that the comparison produces results within the uncertainty in the data (Huber and Caballero, 2011; Lunt et al., 2012). What we suspect now is that most modeling work of the past three decades was probably missing the mark in regard to heat transport, largely because their targeted global mean temperatures were too low and the nonlinear feedbacks that help to decrease meridional-temperature gradients, such as those that impact Hadley Cell width and poleward latent-heat transport, were not accessible in older models.

If future global warming simulations are used as a guide, a warmer world should be characterized by an intensified hydrological cycle and a slightly increased Hadley Cell width, with storm tracks displaced poleward by 2–3° latitude (Frierson et al., 2007; Lu et al., 2007; Seager et al., 2007). But for the Eocene and Cretaceous greenhouse, Hadley Cell width could have shifted by 5–8° in latitude (based on the scaling of Frierson et al. (2007)) with an associated shift in storm tracks, and major regions of hydrological and water isotope divergence. This supposition could be testable with paleoclimate proxy data, but a subtle signal could be hard to discern with sparsely distributed proxy data localities. However, it should be possible to qualitatively determine an increase in the hydrological cycle during greenhouse times, which would be an important clue in explaining warm, low-gradient climates.

The characterization of 'wet' Eocene and Cretaceous conditions is readily interpreted as reflecting an enhanced hydrological cycle in a wetter world (Bowen et al., 2004; Greenwood et al., 2010; Wilf et al., 1998). However, a 'more intense' hydrological cycle refers to increased meridional water-vapor transport from low- to high latitudes. Assuming steady-state conditions, this requires an intensification of evaporation in 'zones of net-evaporation' and a counterbalancing increase in precipitation in 'zones of net-precipitation.' This leads to an increased meridional gradient of evaporation over precipitation (Allen and Ingram, 2002; Held and Soden, 2006), consistent with climate simulations of future warming that show a general drying of the subtropics (and moistening of the deep tropics and high latitudes). The first-order effect in the net-surface fresh-water flux during global warming is a simple amplification without a change in the spatial pattern. Under steady-state conditions, there must be excess precipitation averaged over the extratropics provided that evaporation exceeds precipitation equatorward of the subtropical margins (and the work of Ziegler et al., 2003 suggests that this has been the case since the Permian). Thus, drying (or salinification) of the subtropical regions is consistent with an increase in the strength of the hydrological cycle with a compensating moistening in high latitudes. In other words, during times with a more intense hydrological system, some regions must get drier or more saline (in addition to the enhanced effective moisture in extra-tropical regions normally noted in paleoclimate proxy studies) to support increased hydrological cycles and latent-heat transport elsewhere. This pattern appears to be playing itself out in modern hydrological records (Zhang et al., 2007), and some evidence indicates that a similar result occurred during Eocene hyperthermals (Pagani et al., 2006a), but conclusions are not firm, in large part because adequate records showing subtropical drying or salinification have not be found.

Sediments recovered from the central Arctic Ocean provided the first opportunity to directly evaluate the environmental response at the North Pole during intense warming (Moran et al., 2006). Stable hydrogen (δD) and carbon ($\delta^{13}C$) isotope measurements of waxes derived from terrestrial- and aquatic plants show substantial changes in hydrology, including surface water salinity and precipitation, and suggest that Arctic PETM precipitation was D-enriched relative to today, with hydrogen isotopic compositions comparable with modern, mid-latitude precipitation (Pagani et al., 2006a).

D-enriched Arctic precipitation during the PETM could have resulted from two possible end-member processes, including changes in proximal evaporative sources or a decrease in large-scale (hemispheric to global) meridional (or vertical) temperature gradients. Changes in evaporative sources large enough to explain the observed δD shift during the PETM would require a fundamental, global alteration in precipitation and evaporation. However, such effects are not supported by physical modeling or proxy data. The preferable model is that decreased meridional and/or vertical temperature gradients conspired to reduce rainout of subtropical water vapor by synoptic eddies (Caballero and Langen, 2005), decreased isotopic distillation during vapor transport, and lead to D-enriched precipitation at high latitudes. If surface temperature gradients remained constant during the PETM, then changes in atmospheric static stability could have decreased rainout in the mid-latitudes (e.g., Pagani et al. 2006a). In either case, a decrease in temperature gradients should be expressed as a reduction in the meridional isotopic gradient of precipitation. Because a reduced meridional isotopic gradient implies less rainout along an airmass's trajectory, more water vapor must have been transported to extreme high latitudes. This view was supported by an analysis of Arctic Ocean surface water salinity reconstructed from the hydrogen isotope composition of aquatic biomarkers, which indicated that Arctic Ocean surface water salinity decreased as the PETM evolved, followed by a rapid increase in salinity toward the end of the climate anomaly (Pagani et al., 2006a). These interpretations were further corroborated by the presence of low-salinity tolerant dinocyst assemblages and the occurrence of isorenieratene derivatives biomarkers indicative of anoxia within the photic zone (Sluijs et al., 2006; Stein et al. 2006). Termination of these conditions and a progressive change to fewer low-salinity tolerant dinocyst assemblages (Sluijs et al., 2006) coincided with a trend toward more saline surface waters by the end of the climate anomaly. This scenario suggests that the latitude of maximum latent-heat flux divergence (today at ~40°) shifted closer to the poles during the initial warming of the PETM, consistent with theory.

Enhanced moisture and latent-heat transport from the subtropics to the Arctic region could have resulted from the nonlinear dependence of the saturation-specific humidity of subtropical air parcels as a function of temperature, and/or at the expense of mid-latitude precipitation. The primary sources of atmospheric water vapor derive from the tropical and subtropical ocean. Poleward and altitudinal advection of air parcels approximately along isentropic surfaces (Pierrehumbert, 1998) leads to cooling, condensation, an increase in the isotopic fractionation between the vapor and the condensate, and progressive isotopic distillation resulting in D-depleted high-latitude precipitation (Noone, 2008). Thus, it is possible that the subtropics and parts of the mid-latitudes experienced less net precipitation during the PETM if the modern observed pattern (Seager et al., 2007; Zhang et al., 2007a,b,c) held true in the past (Pagani et al., 2006a). This remains to be proven, but preliminary work (Bowen and Bowen, 2008; Kraus and Riggins, 2007; Wing et al., 2005) is supportive.

6.13.6.4 The Role of Vegetation

Equally perplexing as the appearance of low thermal gradients, is the evidence for very low seasonality and above-freezing conditions that characterize continental interiors far from the mediating force of a warm ocean (Eberle et al., 2010; Greenwood and Wing, 1995; Herman and Spicer, 1996; Markwick, 2007; Sloan, 1994; Sloan and Barron, 1990; Spicer and Parrish, 1990; Spicer et al., 2008; Upchurch et al., 1999; Wolfe, 1980, 1994). Unlike oceans, the interiors of large continents have low heat capacities and climate is largely modulated by the seasonal solar cycle. Moreover, low meridional-temperature gradients would further reduce atmospheric advection, making the appearance of equable continental conditions more difficult to explain (Sloan and Barron, 1990). Even if additional and undetermined ocean heat transport mechanisms were in play that reduced meridional gradients, ocean heat would do little to ameliorate continental interiors (Huber and Sloan, 1999; Sewall et al., 2004; Sloan et al., 2001). This 'low-gradient problem' persists in models at atmospheric carbon dioxide boundary conditions up to $\sim$2000 ppm, where model-data mismatch is typically $\sim$20 °C for winter temperatures (Shellito et al., 2003).

Part of the solution for equable continental climates can be potentially explained by paleogeography, which can reduce winter temperatures through enhanced latent-heat transport (Donnadieu et al., 2006), but given that this is already incorporated in climate models the continuation of model-data mismatch indicates that this is not the primary cause. Another part of the solution rests on the visualization of vast, globally expansive forested ecosystems that span to the poles. The advent of more complex GCMs coupled to vegetation models provide evidence that low continental seasonality is linked to the role that vegetation plays in modulating regional and global climate (Boyce and Lee, 2010; DeConto et al., 1999; Otto-Bliesner and Upchurch, 1997; Upchurch et al., 1999). Greenhouse vegetation substantially reduces albedo and enhances latent-heat flux through transpiration effects (DeConto et al., 1999). While promoting lower latitudinal gradients, vegetation substantially impacts continental climates as warmer interiors lead to lower surface pressures and atmospheric convergence that drives the advection of warm, moist ocean air (DeConto et al., 1999). Unfortunately, vegetation distributions derived from paleobotanical observations still produce temperatures much too cold (Sewall et al., 2000).

While vegetation is clearly important, a satisfactory explanation for the appearance of warm winter continental interiors and polar temperatures remains vexing. A range of other factors have been considered including the effects of large lakes (Morrill et al., 2001; Sloan, 1994), polar stratospheric clouds (Kirk-Davidoff and Lamarque, 2008; Kirk-Davidoff et al., 2002; Peters and Sloan, 2000; Sloan and Pollard, 1998; Sloan et al., 1992, 1999), increased ocean heat transport (Barron et al., 1993; Covey and Barron, 1988; Sloan et al., 1995), finer resolution simulations of continental interiors (Sewall and Sloan, 2006; Thrasher and Sloan, 2009), a permanent, positive phase of the Arctic Oscillation (Sewall and Sloan, 2001), altered orbital parameters (Lawrence et al., 2003; Sewall and Sloan, 2004; Sloan and Morrill, 1998), altered topography and ocean gateways (Sewall et al., 2000; Shellito et al., 2009), radiative convective feedbacks (Abbot et al., 2009), altered vegetation (Sewall et al., 2000; Shellito and Sloan, 2006a,b), changes in SST distributions (Huber and Sloan, 1999; Sewall et al., 2004; Sloan et al., 2001), and cloud droplet dimensions and their influence on planetary albedo (Kump and Pollard, 2008).

While some regions have proven sensitive to variations in these climate-forcing mechanisms, the general outcome of model investigations has been failure to provide a general solution to the equable climate problem. One mechanism might explain warmth at extreme high latitudes (e.g., cloud feedbacks), but leave temperatures within the western interior of North America unexplained (e.g., large lakes or altered topography). Ultimately, failure of these various hypothesized resolutions to the 'low-gradient problem' – whether tested individually or in concert – suggests that they are not the leading solution to the problem. However, recent advances have been made (Lunt et al., 2012), and progress is paradoxically linked to the recognition of higher temperature estimates and consideration of atmospheric carbon dioxide concentrations (Huber and Caballero, 2011).

6.13.7 Estimates of Atmospheric Carbon Dioxide in Relationship to Greenhouse Climates

Irrefutable evidence for the role of diagenesis in driving the appearance of cool tropical SSTs (Pearson et al., 2001) has now dispelled the notion that heat redistribution was the primary cause of equable greenhouse conditions. But prior to that conclusion, early climate simulations recognized the need for additional sources of heat in order to come to terms with the overall warmth of the Cretaceous (Barron et al., 1981). Greenhouse gases were long suspected as the agent driving greenhouse/icehouse climates, but results from the BLAG geochemical model (Berner et al., 1983) and organic isotopic arguments (Arthur et al., 1985) renewed support for carbon dioxide as a primary mover and helped spur a generation of simulations exploring the importance of CO_2 on climate (e.g., Barron and Washington, 1985).

Explaining patterns in Earth's CO_2 history remains a major scientific challenge. Over long-time scales, atmospheric CO_2 concentrations evolve in response to changes in the rates of carbon outgassing due to volcanism or metamorphic decarbonation and carbon removal through the coupling of silicate chemical weathering and carbonate burial (Berner, 1991, 1994; Berner and Kothavala, 2001; Berner et al. 1983). Geochemical model refinements (Berner, 1991, 2006) and new isotope proxies (Cerling, 1991; Fletcher et al., 2008; Freeman and Hayes, 1992; Lowenstein and Demicco, 2006; Pagani et al., 2005; Popp et al., 1989) continue to call on higher CO_2 levels associated with warmer climates. Further, higher CO_2 levels in all paleomodel exercises substantially improve simulated global temperatures relative to proxy estimates.

The emergence of new CO_2 proxies provided qualitative and quantitative support for the influence of greenhouse gases on climate (Arrhenius, 1896; Plass, 1956). Higher Cretaceous and early Tertiary CO_2 levels were broadly inferred from the stable carbon isotopic composition of marine organic carbon (Arthur et al., 1985) and porphryin-based reconstructions of the total carbon isotope fractionation occurring during marine photosynthesis (ε_p) (Popp et al., 1989). Quantitative CO_2 estimates of porphryin-derived ε_p values followed (Freeman and Hayes, 1992), providing support for CO_2 levels over 800 ppm during peak warming in the middle Cretaceous, with near-modern values occurring sometime in the Miocene. Stable carbon isotope compositions of pedogenic carbonates were also shown to reflect the partial pressure of atmospheric CO_2 (Cerling, 1991) and provided somewhat similar results, with very high CO_2 concentration during the late Triassic (2000–4000 ppmv) and early Cretaceous (1500–3000 ppmv). A subsequent higher resolution soil-carbonate CO_2 study indicates the potential of a broad maximum in atmospheric CO_2 during the Mesozoic and the early Eocene, peaking at >3000 and >1500 ppmv, respectively (Ekart et al., 1999), with minimum values <1500 to ~500 ppm for the latest Cretaceous (Andrews et al., 1995; Ekart et al., 1999). Similar patterns of pCO_2 change have been recently reconstructed using the carbon isotopic composition of nonvascular plant (bryophyte) organic matter (Fletcher et al., 2008). This methodology is similar to techniques developed for algal ε_p values because bryophytes do not contain stomata and rely on a diffusive delivery of CO_2 for carbon fixation.

Background CO_2 conditions for the Eocene were substantially higher than today and the relationship between CO_2 levels and the heat of greenhouse climates is increasingly clear (Beerling and Royer, 2011) (**Figure 9**). Alkenone-based CO_2 estimates (Pagani et al., 2005) and other algal isotope proxies (Freeman and Hayes, 1992) show a trajectory of increasing CO_2 levels from the late Eocene toward the Early Eocene Climatic Optimum, consistent with the CO_2 range implied by the stability of the sodium carbonate nacholite found in the Green River Formation (Lowenstein and Demicco, 2006) and one record derived from bryophyte carbon isotope chemistry (Beerling and Royer, 2011; Fletcher et al., 2008), but substantial disagreements persist for the height of warming during the early Eocene. CO_2 estimates established from fossil leaf stomata indices (Doria et al., 2011; Haworth et al., 2005; Royer, 2003) provide some of the lowest CO_2 values for the Cretaceous and Eocene.

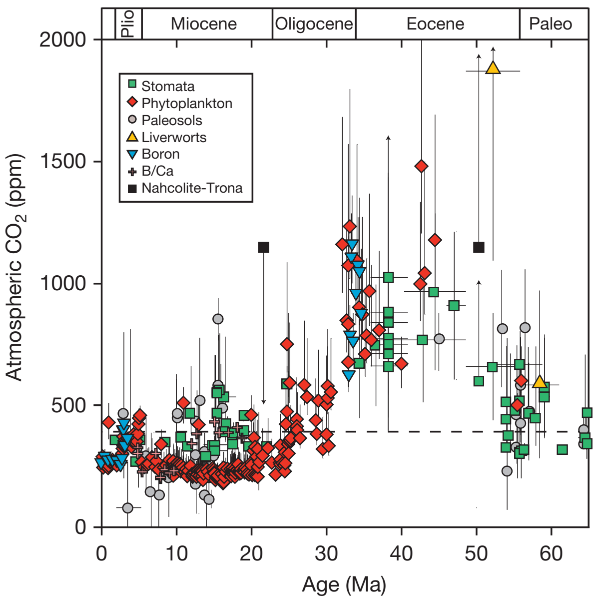

Figure 9 Proxy estimates of Cenozoic atmospheric CO_2 (modified from Beerling DJ and Royer DL (2011) Convergent Cenozoic CO_2 history. *Nature Geoscience* 4: 418–420). Errors represent reported uncertainties. Symbols with arrows indicate either upper or lower limits. Magnitudes of CO_2 reflect recently revised calibrations. Dashed line is modern (year 2012) CO_2 concentrations of 390 ppm.

Recently, CO_2 values derived from the carbon isotopic composition of soil-carbonate nodules have been downgraded by ~50% (Beerling and Royer, 2011; Breecker et al., 2010; Hong and Lee, 2012) in consideration of the seasonality of nodule formation and soil CO_2 content as reflected in modern settings (Breecker et al., 2009), and leaf stomata estimates have been elevated as a result of statistical treatments (Beerling et al., 2009). These new paleosol CO_2 estimates appear to result in a convergence of CO_2 values with species-specific stomata index estimates of ≤1000 ppm for the early Eocene (Beerling and Royer, 2011) and the Cretaceous (Quan et al., 2009) (**Figure 10**).

While some argue that the newly revised data reflect an increasing consensus for paleo-CO_2 proxies during the Cenozoic (Beerling and Royer, 2011), the legitimacy of the CO_2 range expressed by the existing data during peak warming is an area of active debate. Error bars for CO_2 estimates remain large and the resolution of many data sets precludes assessment of shorter-term variability. The lowest CO_2 values during the height of the Eocene greenhouse climate warming lead to several possible implications including (1) a very strong role for greenhouse gases other than CO_2, which increase with increasing CO_2 concentrations (Beerling et al. 2011), (2) a substantial increase in global temperature due to paleogeography, or (3) a high climate sensitivity to CO_2. The application of relatively low soil-respired CO_2 values across all paleosol nodule data that recently pushed calculated CO_2 values downward is contentious and subject to challenge (Montañez, 2013). Further, the stomatal index (SI) methodology used to estimate paleo-CO_2 is potentially impacted by irradiance and nutritional constraints among other things and varies among modern species for a given pCO_2 (Atchison et al., 2000; Franks and Beerling, 2009; Wagner et al., 2000). Some near-modern records show SI trends with increasing CO_2 that oppose theory (Atchison et al., 2000) and suggest other leading environmental factors as a control on SI. For those modern species (e.g., *Ginkgo biloba*) with limited genetic and environmental ranges that show consistent experimental and empirical relationships with CO_2 change, ancient leaf CO_2 records assume no evolutionary adaptation, even though these fossils were likely part of a more genetically diverse group given their broader geographical range in the past (Jordan, 2011). These evolutionary concerns coupled with the strong asymptotic relationship between SI and CO_2 at relatively low pCO_2 concentrations (e.g., 400–500 ppm; Beerling et al., 2009) add considerable uncertainty to the upper limits of CO_2 during peak greenhouse conditions of the Cretaceous and Eocene (Jordan, 2011).

6.13.7.1 Greenhouse CO_2 and Climate Sensitivity

Past failures to simulate the temperature characteristics of greenhouse climates represent one of the greatest challenges in paleoclimate modeling because they suggest that climate models cannot reproduce the leading order feedbacks in a warmer

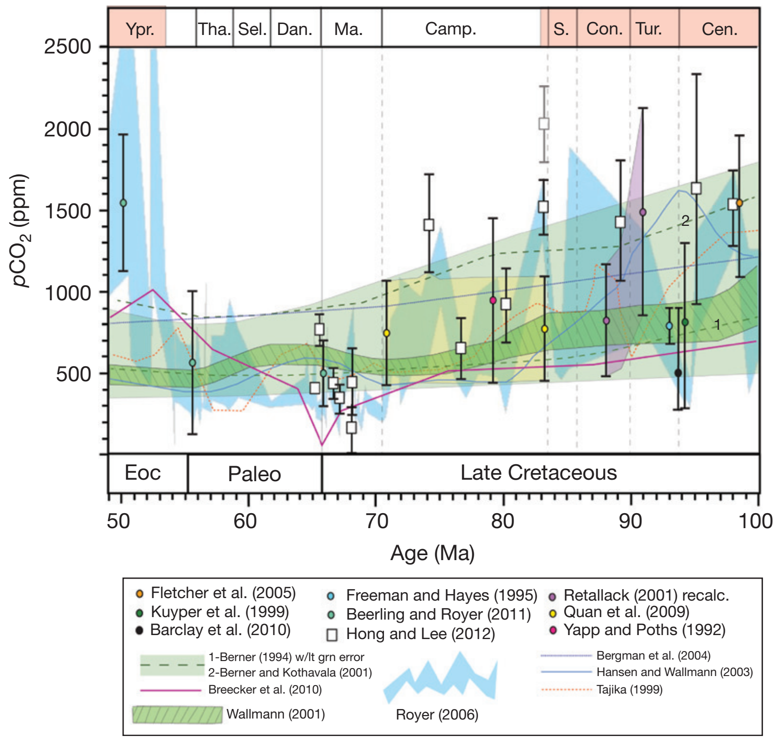

Figure 10 A compilation of paleo-pCO_2 for 50–100 Ma includes selected proxy data (paleobotanical and C-isotope techniques) and revised estimates (Breecker et al., 2010; Ekart et al., 1999; Hong and Lee, 2012; Montañez et al., 2007; Quan et al., 2009; Royer, 2006), as well as geochemical model estimates (see key for citations). The lighter colored high pCO_2 value from Hong and Lee (2012) in the Early Campanian reflects an alternate calibration of the proxy method based on paleosol C-isotopes. The reddish bands in the upper part of the figure mark the periods of elevated pCO_2 based on proxy data and correspond to Cretaceous and Eocene hyperthermals, defined arbitrarily as intervals with multiple proxy estimates near 1500 ppm and upper errors near or above 2000 ppm (note that this definition extends the duration of the Cretaceous hyperthermal into the early Campanian). Note that the Royer (2006) compilation represented by the blue envelope includes some of the data points from the other studies, as well as additional data, mostly from stomatal index.

world. Unless models of stellar evolution are greatly revised, higher greenhouse gasses are the only known variables that explain a hotter Earth under a younger, cooler sun (Pavlov et al., 2000; Sagan and Mullen, 1972). Atmospheric pCO_2 is generally considered to play both primary and secondary roles in explaining global warmth of greenhouse conditions (e.g., high CO_2 concentrations could have enhanced nonlinear sensitivity through feedbacks). How much CO_2 is required to explain average global temperatures of the Cretaceous and Eocene, as well as the role that other infrared-active trace gases play, resides at the heart of the current debate for both greenhouse climates and future climate projections (Lowenstein and Demicco, 2006; Pagani et al., 2005; Pearson and Palmer, 2000; Royer, 2003, 2006).

The potential impact of CO_2 on solving the leading temperature characteristics of greenhouse climates has not been adequately explored because modelers often select conservative estimates (520–2200 ppm) of paleo-pCO_2 even though they potentially extend up to 4400 ppm during the early Eocene (Zachos et al., 2008). Conservatism is driven, in part, by older model results that produced tropical SSTs warmer than tropical reconstructions with pCO_2 above 2000 ppm (Shellito et al., 2003). Paleoclimate simulations with high CO_2 boundary conditions often exhibit the competing interests of warming-up winter temperatures in continental interiors without overheating the tropics. However, tropical SST reconstructions have been revised upwards as discussed previously (Pearson et al., 2007).

CO_2 concentrations higher than some proxy records suggest are valid experimental boundary conditions because the global-mean temperature response to greenhouse gases (i.e., the equilibrium sensitivity of temperature to a doubling of pCO_2) is poorly constrained (Knutti and Hegerl, 2008; Roe and Baker, 2007). Highly probable estimates for equilibrium sensitivity (S) under modern-day conditions range from 2.5 to 4.5 °C, but a much broader range is possible. The range implied by paleoclimate conditions is similar, although perhaps leans toward the higher end of the range and includes feedbacks that occur on long-time scales not considered in equilibrium sensitivity estimates (Pagani et al., 2006a, 2009; Park and Royer, 2011).

The value of S is an emergent property of any given climate model – it is not directly specified and nontrivial to adjust. Consequently, even if CO_2 levels in the past were perfectly known, it would still be necessary to use a climate model with the correct sensitivity value or to adjust the input value of CO_2 until the correct global MAT was achieved. For example, if the true value of S is 6 °C per CO_2 doubling and a climate model expresses S equivalent to 3 °C per doubling, then twice the value of CO_2 would be required to approach accurate solutions.

A recent comparison of early Eocene simulations produced by different models (using CO_2 ranging from 560 to

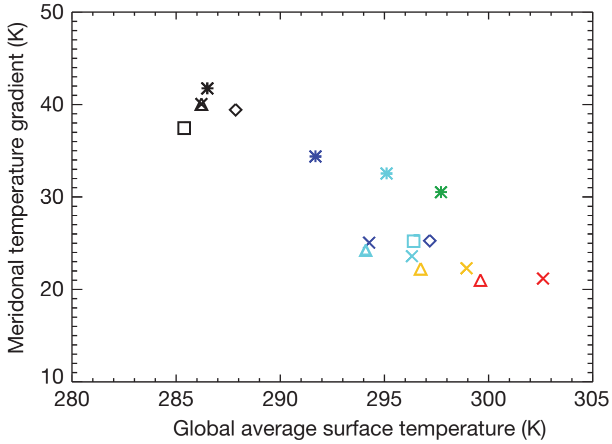

Figure 11 Equator-to-pole temperature gradient as a function of global mean surface temperature in a suite of different coupled climate models. The different symbol shapes refer to different models whereas the different colors reflect different CO_2 levels. Temperature gradient diminishes with global mean temperatures for any individual model and also the same trend is noted across all the models. Polar amplification increases with global mean temperature. Modified from Lunt DJ, Jones TD, Heinemann M, et al. (2012) A model-data comparison for a multimodel ensemble of early Eocene atmosphere–ocean simulations: EoMIP. *Climates of the Past* 8: 1229–1273.

4480 ppmv) indicates that the application of very high pCO_2 boundary conditions results in good agreement between proxy temperatures and model outputs (Lunt et al., 2012), and begins to solve the classic 'low-gradient problem' of greenhouse climates (**Figure 11**). All climate models to date require a pCO_2 concentration of at least 1000 ppm to be in reasonable agreement with proxy records of high-latitude- and deep-ocean warmth, or the new warmer interpretations of tropical SSTs during greenhouse conditions (Lunt et al., 2012). One interpretation is that much higher levels of CO_2 than previously assumed are necessary to approach peak warming of greenhouse states, and some proxy data support this view. For example, early Eocene CO_2 estimates based on the appearance of nacholite (Lowenstein and Demicco, 2006) and liverwort geochemistry (Beerling and Royer, 2011) that allow for a pCO_2 estimate of $\sim$2000 ppm might be correct. This does not necessarily mean that the solution to the peculiarities of greenhouse temperature distributions is simply very high CO_2 concentrations (or other well-mixed greenhouse gases). The heart of the problem could also reside in the emergent value of equilibrium climate sensitivity (or *S*) for each model and, if valid this suggests that climate models exhibit values of *S* that are too low or lack an accurate representation of positive feedbacks associated with Earth System climate sensitivity. The most recent model results are encouraging (**Figure 12**) (Huber and Caballero, 2011; Lunt et al., 2012) and if an accurate value

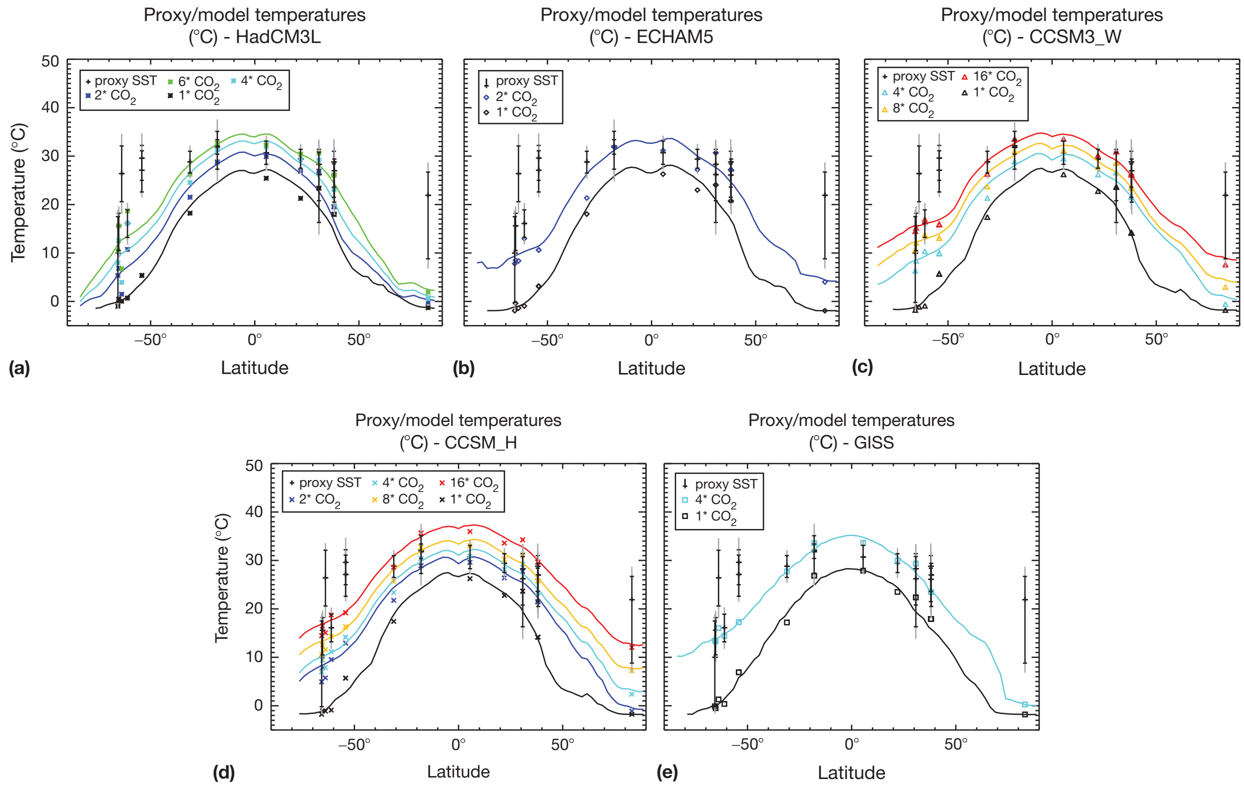

Figure 12 Comparison of SST proxies and coupled climate model results. Each colored line represents the zonal mean SST for a range of CO_2 values indicated in the figure legend. Five models and model configurations are shown in this panel figure (HadCM3L, ECHAM5, CCSM3_W, CCSM_H, and GISS) as indicated at the top of each figure. The symbols represent proxy reconstructed SST and modeled values at the same location. The color of the symbols reflect CO_2 values as indicated by the figure legend. CCSM_H (described in Huber and Caballero, 2011) produces the best fit with proxies, but 4480 ppm CO_2 is required. Modified from Lunt DJ, Jones TD, Heinemann M, et al. (2012) A model-data comparison for a multimodel ensemble of early Eocene atmosphere–ocean simulations: EoMIP. *Climates of the Past* 8: 1229–1273.

of S for any particular model can be constrained, then the temperature change could be determined if pCO_2 was known. However, an accurate representation of greenhouse climates clearly remains a work in progress.

6.13.8 Summary

Much of what we expect to be associated with warmer conditions – higher atmospheric carbon dioxide levels and enhanced hydrological effects – are confirmed in proxy records during greenhouse climates. However, better quantifications will require further advancements and confidence in ocean pH and CO_2 proxies, and SST distributions. Recent advancements in temperatures proxies and development of paleoclimate records call for even warmer tropical and high-latitude temperatures than originally surmised.

Three main characteristics appear to define these warm climate states including: (1) global warmth with global mean surface temperatures much warmer than the modern global mean temperature (15 °C), (2) equable climates characterized by reduced seasonality in continental interiors compared to modern, with winter temperatures above freezing, and (3) substantially smaller equator-to-pole and vertical ocean temperature gradients. Proxy records also support the appearance of an invigorated hydrologic system during warmer conditions, consistent with expectations. Although some evidence and arguments for episodic, and perhaps periodic, glaciation have been presented for very warm intervals, conclusive proof of their occurrence is wanting.

All climate models predict that low-latitude temperatures increase under higher CO_2 levels. However, while an overly hot tropical realm with higher CO_2 was initially viewed as a problem in early experiments, the most recent proxy temperatures now call for higher tropical temperatures than previously reconstructed and challenge the notion that tropical temperatures were buffered by difficult-to-explain natural thermostats (Pierrehumbert, 1995).

Low equator-to-pole temperature gradients during greenhouse climates continue to be vexing and inadequately simulated in the current generation of climate models, particularly when only moderately high CO_2 boundary levels are assumed. However, solutions could be just over the horizon. Recent model assessments suggest that greenhouse climate simulations best match temperature proxy data when substantially higher CO_2 levels are applied. This suggests that proxies have substantially underestimated the magnitude of radiative forcing associated with peak greenhouse conditions or that important positive climate feedbacks in models are lacking that lower climate sensitivity and inhibit an accurate representation of greenhouse conditions. In either case, the true impact of greenhouse gas-induced global warming remains a work in progress.

References

Abbot DS, Huber M, Bousquet G, and Walker CC (2009) High-CO_2 cloud radiative forcing feedback over both land and ocean in a global climate model. *Geophysical Research Letters* 36. http://dx.doi.org/10.1029/2008GL036703.

Adams DD, Hurtgen MT, and Sageman BB (2010) Volcanic triggering of a biogeochemical cascade during Oceanic Anoxic Event 2. *Nature Geoscience* 3. http://dx.doi.org/10.1038/ NGEO743

Agnini C, Muttoni G, Kent DV, and Rio D (2006) Eocene biostratigraphy and magnetic stratigraphy from Possagno, Italy: The calcareous nannofossil response to climate variability. *Earth and Planetary Science Letters* 241: 815–830.

Alexandre TJ, Tuenter E, Henstra GA, et al. (2010) Mid-Cretaceous North Atlantic nutrient trap: Black shales and OAEs. *Paleoceanography* 25. http://dx.doi.org/10.1029/2010PA001925.

Al-Hajari S and Khaled KA (1994) Lower Eocene black shale beds of Rus formation in north of Oman – Possible oil shales. *Qatar University Science Journal* 14: 368–372.

Allen MR and Ingram WJ (2002) Constraints on future changes in climate and the hydrologic cycle. *Nature* 419: 224–232.

Alley NF and Frakes LA (2003) First known Cretaceous glaciation: Livingston Tillite member of the Cadnaowie Formation, South Australia. *Australian Journal of Earth Sciences* 50: 139–144.

Ando A, Huber BT, MacLeod KG, Ohta T, and Khim B-K (2009) Blake Nose stable isotopic evidence against the mid-Cenomanian glaciation hypothesis. *Geology* 37: 451–454.

Andrews JE, Tanden SK, and Dennis PF (1995) Concentration of atmospheric carbon dioxide in the late Cretaceous atmosphere. *Journal of the Geological Society of London* 152: 1–3.

Archer D and Buffett B (2005) Time-dependent response of the global ocean Clathrate reservoir to climatic and anthropogenic forcing. *Geochemistry, Geophysics, Geosystems* 6: Q03002.

Archer D, Martin P, Buffett B, Brovkin V, Rahmstorf S, and Ganopolski A (2004) The importance of ocean temperature to global biogeochemistry. *Earth and Planetary Science Letters* 222: 333–348.

Arrhenius S (1896) On the influence of carbonic acid in the air upon the temperature of the ground. *Philosphical Magazine* 41: 237–276.

Arthur MA, Dean WE, and Claypool GE (1985) Anomalous ^{13}C enrichment in modern marine organic carbon. *Nature* 315: 216–218.

Arthur MA, Dean WE, and Pratt LM (1988) Geochemical and climatic effects of increased marine organic carbon burial at the Cenomanian/Turonian boundary. *Nature* 335: 714–717.

Askin RA (1990) Campanian to Paleocene spore and pollen assemblages of Seymour Island, Antarctica. *Review of Palaeobotany and Palynology* 65: 105–113.

Atchison JM, Head LM, and McCarthy LP (2000) Stomatal parameters and atmospheric change since 7500 years before present: Evidence from *Eremophila deserti* (Myoporaceae) leaves from the Flinders Ranges region, South Australia. *Australian Journal of Botany* 48: 223–232.

Axelrod DI (1984) An interpretation of Cretaceous and Tertiary biota in Polar regions. *Palaeogeography, Palaeoclimatology, Palaeoecology* 45: 105–147.

Barclay RS, McElwain JC, and Sageman BB (2010) Volcanic CO_2 pulse activates carbon sequestration during Cretaceous Oceanic Anoxic event 2. *Nature Geoscience* 3: 205–208.

Barrera E, Huber BT, Savin SM, and Webb PN (1987) Antarctic marine temperatures: Late Campanian through early Paleocene. *Paleoceanography* 2: 21–47.

Barron EJ (1983) A warm, equable Cretaceous: The nature of the problem. *Earth-Science Reviews* 19: 305–338.

Barron EJ (1987) Eocene equator-to-pole surface ocean temperatures: A significant climate problem? *Paleoceanography* 2: 729–739.

Barron EJ, Peterson WH, Thompson SL, and Pollard D (1993) Past climate and the role of ocean heat transport: Model simulations for the Cretaceous. *Paleoceanography* 8: 785–798.

Barron EJ, Sloan JL, and Harrison CGA (1980) Potential significance of land–sea distribution and surface albedo variations as climatic forcing factor: 180 M.Y. to the present. *Palaeogeography, Palaeoclimatology, Palaeoecology* 30: 17–40.

Barron EJ, Thompson SL, and Schneider SH (1981) An ice-free Cretaceous? Results from climate model. *Science* 212: 501–508.

Barron EJ and Washington WM (1982) Atmospheric circulation during warm geologic periods: Is the equator-to-pole surface temperature gradient the controlling factor? *Geology* 10: 633–636.

Barron EJ and Washington WM (1984) The role of geographic variables in explaining paleoclimates results from Cretaceous climate model sensitivity studies. *Journal of Geophysical Research* 89: 1267–1279.

Barron EJ and Washington WM (1985) Warm Cretaceous climates: High atmospheric CO_2 as a plausible mechanism. In the carbon cycle and atmospheric CO_2: Natural variations Archean to present. *Geophysical Monograph* 32: 546–553.

Basinger JF, Greenwood DR, and Sweda T (1994) Early tertiary vegetation of Arctic Canada and its relevance to paleoclimatic interpretation. In: Boulter MC and Fisher HC (eds.) *Cenozoic Plants and Climate of the Arctic*. NATO ASI Series, pp. 175–198. Berlin: Springer-Verlag.

Beerling DJ, Berner RA, Mackenzie FT, Harfoot MB, and Pyle JA (2009) Methane and the CH_4-related greenhouse effect over the past 400 million years. *American Journal of Science* 309: 97–115.

Beerling DJ, Fox A, Stevenson DS, and Valdes PJ (2011) Enhanced chemistry-climate feedbacks in past greenhouse worlds. *Proceedings of the National Academy of Sciences* 108: 9770–9775.

Beerling DJ and Royer DL (2011) Convergent Cenozoic CO_2 history. *Nature Geoscience* 4: 418–420.

Bennett MR and Doyle P (1996) Global cooling inferred from dropstones in the Cretaceous: Fact or wishful thinking? *Terra Nova* 8: 182–185.

Berner RA (1991) A model for atmospheric CO_2 over the Phanerozoic time. *American Journal of Science* 291: 339–376.

Berner RA (1994) GEOCARB II: A revised model of atmospheric CO_2 over Phanerozoic time. *American Journal of Science* 294: 56–91.

Berner RA (2006) GEOCARBSULF: A combined model for Phanerozoic atmospheric O_2 and CO_2. *Geochimica et Cosmochimica Acta* 70: 5653–5664.

Berner RA and Kothavala Z (2001) GEOCARB III: A revised model of atmospheric CO_2 over Phanerozoic time. *American Journal of Science* 301: 182–204.

Berner RA, Lasaga AC, and Garrels RM (1983) The carbonate–silicate geochemical cycle and its effect on atmospheric carbon dioxide over the last 100 million years. *American Journal of Science* 283: 641–683.

Berry EW (1922) A possible explanation of upper Eocene climates. *Proceedings of the American Philosophical Society* 61: 1–14.

Bice KL, Birgel D, Meyers PA, Dahl KA, Hinrichs K-U, and Norris RD (2006) A multiple proxy and model study of Cretaceous upper ocean temperatures and atmospheric CO_2 concentrations. *Paleoceanography* 21: PA2002.

Bice KL, Huber BT, and Norris RD (2003) Extreme polar warmth during the Cretaceous greenhouse? Paradox of the late Turonian $\delta^{18}O$ record at Deep Sea Drilling Project Site 511. *Paleoceanography* 18. http://dx.doi.org/10.1029/2002PA000848.

Bice KL and Marotzke J (2001) Numerical evidence against reversed thermohaline circulation in the warm Paleocene/Eocene ocean. *Journal of Geophysical Research* 106: 11529–11542.

Bijl PK, Houben AJP, Schouten S, et al. (2010) Transient middle Eocene atmospheric CO_2 and temperature variations. *Science* 330: 819–821.

Blanz T, Emeis K-C, and Siegel H (2005) Controls on alkenone unsaturation ratios along the salinity gradient between the open ocean and the Baltic Sea. *Geochimica et Cosmochimica Acta* 69: 3589–3600.

Bornemann A, Norris RD, Friedrich O, et al. (2008) Isotopic evidence for glaciation during the Cretaceous supergreenhouse. *Science* 319: 189–192.

Boucsein B and Stein R (2009) Black shale formation in the late Paleocene/early Eocene Arctic Ocean and paleoenvironmental conditions: New results from a detailed organic petrological study. *Marine and Petroleum Geology* 26: 416–426.

Boulila S, Galbrun B, Laskar J, and Pälike H (2012) A 9 myr cycle in Cenozoic $\delta^{13}C$ record and long-term orbital eccentricity modulation: Is there a link? *Earth and Planetary Science Letters* 317–318: 273–281.

Bowen GJ, Beerling DJ, Koch PL, Zachos JC, and Quattlebacum T (2004) A humid climate state during the Palaeocene/Eocene thermal maximum. *Nature* 432: 495–499.

Bowen GJ and Bowen BB (2008) Mechanisms of PETM global change constrained by a new record from central Utah. *Geology* 36: 379–382.

Boyce CK and Lee J-E (2010) An exceptional role for flowering plant physiology in the expansion of tropical rainforests and biodiversity. *Proceedings of the Royal Society B* 277: 3437–3443.

Bralower TJ (2002) Evidence of surface water oligotrophy during the Paleocene–Eocene thermal maximum: Nannofossil assemblage data from Ocean Drilling Program Site 690, Maud Rise, Weddell Sea. *Paleoceanography*. http://dx.doi.org/10.1029/2001PA000662.

Breecker D, Sharp ZD, and McFadden L (2009) Seasonal bias in the formation and stable isotope composition of pedogenic carbonate in modern soils from central New Mexico, USA. *Geological Society of America Bulletin* 121: 630–640.

Breecker DO, Sharp ZD, and McFadden LD (2010) Atmospheric CO_2 concentrations during ancient greenhouse climates were similar to those predicted for A.D. 2100. *Proceedings of the National Academy of Sciences* 107: 576–580.

Brinkhuis H, Sinninghe Damsté JS, Dickens GR, et al. (2006) Episodic fresh surface waters in the Eocene Arctic Ocean. *Nature* 441: 606–609.

Buffett B and Archer DE (2004) Global inventory of methane Clathrate: Sensitivity to changes in environmental conditions. *Earth and Planetary Science Letters* 227: 185–199.

Burton R, Kendall CG, St C, and Lerche I (1987) Out of our depths: On the impossibility of fathoming eustasy from the stratigraphic record. *Earth-Science Reviews* 24: 237–277.

Caballero R and Langen P (2005) The dynamic range of poleward energy transport in an atmospheric general circulation model. *Geophysical Research Letters* 32. http://dx.doi.org/10.1029/2004GL021581.

Cerling TE (1991) Carbon dioxide in the atmosphere: Evidence from Cenozoic and Mesozoic paleosols. *American Journal of Science* 291: 377–400.

Chamberlin TC (1899) An attempt to frame a working hypothesis of the cause of glacial periods on an atmospheric basis. *Journal of Geology* 7: 545–584.

Chamberlin TC (1906) On a possible reversal of deep-sea circulation and its influence on geologic climates. *Journal of Geology* 14: 363–373.

Christie-Blick N, Mountain GS, and Miller KG (1990) Seismic stratigraphic record of sea-level change. In: National Research Council (ed.) *Sea-level Change*, pp. 116–140. Washington, DC: National Academy Press.

Clarke LJ and Jenkyns HC (1999) New oxygen isotope evidence for long-term Cretaceous climatic change in the Southern Hemisphere. *Geology* 27: 699–702.

Coccioni R and Galeotti S (2003) The mid-Cenomanian event: Prelude to OAE2. *Palaeogeography, Palaeoclimatology, Palaeoecology* 190: 427–440.

Conte MH, Thompson A, Lesley D, and Harris RP (1998) Genetic and physiological influences on the alkenone/alkenoate versus growth temperature relationship in *Emiliania huxleyi* and *Gephyrocapsa oceanica*. *Geochimica et Cosmochimica Acta* 62: 51–68.

Covey C and Barron E (1988) The role of ocean heat-transport in climatic change. *Earth-Science Reviews* 24: 429–445.

Cramer BS, Toggweiler JR, Wright JD, Katz ME, and Miller ME (2009) Ocean overturning since the late Cretaceous: Inferences from a new benthic foraminiferal isotope compilation. *Paleoceanography* 24: PA4216.

Creech JB, Baker JR, Hollis CJ, Morgans HEG, and Smith EGC (2010) Eocene sea temperatures for the mid-latitude southwest Pacific from Mg/Ca ratios in planktonic and benthic foraminifera. *Earth and Planetary Science Letters* 299: 483–495.

Crowley T and Zachos JC (2000) Comparison of zonal temperature profiles for past warm time periods. In: Huber BT, MacLeod KG, and Wing SL (eds.) *Warm Climates in Earth History*, pp. 50–76. Cambridge Univ. Press.

Cui Y, Kump LR, Ridgwell AJ, et al. (2011) Slow release of fossil carbon during the Palaeocene–Eocene thermal maximum. *Nature Geoscience* 4: 481–485.

D'Hondt S and Arthur MA (1996) Late Cretaceous oceans and the cool tropic paradox. *Science* 271: 1838–1841.

Davies A, Kemp AES, and Pike J (2009) Late Cretaceous seasonal ocean variability from the Arctic. *Nature* 460: 254–258.

DeConto RM, Galeotti S, Pagani M, et al. (2012) Past extreme warming events linked to massive carbon release from thawing permafrost. *Nature* 484: 87–91.

DeConto RM, Hay WW, Thompson SL, and Bergengren J (1999) Late Cretaceous climate and vegetation interactions: Cold continental interior paradox. In: Barrera E and Johnson CC (eds.) *Evolution of the Cretaceous Ocean-Climate System: Boulder, Colorado, Geological Society of America Special Paper* 332. Boulder, CO: Geological Society of America.

DeConto RM and Pollard D (2003) Rapid Cenozoic glaciation of Antarctica induced by declining atmospheric CO_2. *Nature* 421: 245–249.

DeConto RM, Thompson SL, Pollard D, Brady EC, Bergengren J, and Hay WW (2000) Late Cretaceous climate, vegetation, and ocean interactions. In: Huber BT, MacLeod KG, and Wing SL (eds.) *Warm Climates in Earth History*, pp. 275–296. New York, NY, USA: Columbia University Press.

Demaison GJ and Moore GT (1980) Anoxic environments and oil source bed genesis. *Organic Geochemistry* 2: 9–31.

Dickens GR (2011) Down the rabbit hole: Toward appropriate discussion of methane release from gas hydrate systems during the Paleocene–Eocene thermal maximum and other past hyperthermal events. *Climates of the Past* 7: 831–846.

Dickens GR, O'Neil JR, Rea DK, and Owen RM (1995) Dissociation of oceanic methane hydrate as a cause of the carbon isotope excursion at the end of the Paleocene. *Paleoceanography* 19: 965–971.

Donnadieu Y, Pierrehumbert R, Jacob R, and Fluteau F (2006) Modelling the primary control of paleogeography on Cretaceous climate. *Earth and Planetary Science Letters* 248: 426–437.

Doria G, Royer DL, Wolfe AP, Fox A, Westagate JA, and Beerling DJ (2011) Declining atmospheric CO_2 during the late middle Eocene climate transition. *American Journal of Science* 311: 63–75.

Dorman FH (1966) Tertiary paleotemperatures. *The Journal of Geology* 74: 49–61.

Dorman FH (1968) Some australian oxygen isotope temperatures and a theory for a 30-million-year world-temperature. *Journal of Geology* 76: 297–313.

Douglas RG and Savin SM (1973) Oxygen and carbon isotope analysis of Cretaceous and Tertiary foraminifera from the central north Pacific. *Deep Sea Drilling Program Initial Reports* 17: 591–606.

Douglas RG and Savin SM (1975) Oxygen and carbon isotope analyses of Tertiary and Cretaceous microfossils from Shatsky Rise and other sites in the North Pacific Ocean. *Deep Sea Drilling Program Initial Reports* 32: 509–520.

Dumitresc M, Brassell SC, Schouten S, Hopmans EC, and Sinninghe Damsté JS (2006) Instability in tropical Pacific sea-surface temperatures during the early Aptian. *Geology* 34: 833–836.

Eberle JJ (2005) A new 'tapir' from Ellesmere Island, Arctic Canada—Implications for northern high latitude palaeobiogeography and tapir palaeobiology. *Palaeogeography, Palaeoclimatology, Palaeoecology* 227: 311–322.
Eberle JJ, Fricke HC, Humphrey JD, Hackett L, Newbrey MG, and Hutchinson JH (2010) Seasonal variability in Arctic temperatures during early Eocene time. *Earth and Planetary Science Letters* 296: 481–486.
Eberle JJ and Greenwood DR (2012) Life at the top of the greenhouse Eocene world – A review of the Eocene flora and vertebrate fauna from Canada's High Arctic. *GSA Bulletin* 124: 3–23.
Ekart DD, Cerling TE, Montañez IP, and Tabor N (1999) A 400 million year carbon isotope record of pedogenic carbonate: Implication for paleoatmospheric carbon dioxide. *American Journal of Science* 299: 805–827.
Emanuel KA (2002) A simple model of multiple climate regimes. *Journal of Geophysical Research, Atmosphere* 107. http://dx.doi.org/10.1029/2001JD001002.
Erbacher J, Friedrich O, Wilson PA, Birch H, and Mutterlose J (2005) Stable organic carbon isotope stratigraphy across Oceanic Anoxic Event 2 of Demerara Rise western tropical Atlantic. *Geochemistry, Geophysics. Geosystems* 6: Q06010.
Estes R and Hutchison JH (1980) Eocene lower vertebrates from Ellesmere Island, Canadian Arctic Archipelago. *Palaeogeography, Palaeoclimatology, Palaeoecology* 30: 325–347.
Fischer AG (1981) Climatic oscillations in the biosphere. In: Nitecki MH (ed.) *Biotic Crises in Ecological and Evolutionary Time*, pp. 103–131. New York: Academic Press.
Fischer AG (1982) Long-term climatic oscillations recorded in stratigraphy. In: Berger W (ed.) *Climate in Earth History. National Research Council, Studies in Geophysics*, pp. 97–104. Washington, DC: National Academy Press.
Fischer AG and Arthur MA (1977) Secular variations in the pelagic realm. In: Cook HC and Enos P (eds.) *Deep Water Carbonate Environments. SEPM Special Publication 25*, pp. 18–50. Tulsa: SEPM.
Fjeldskaar W (1989) Rapid eustatic changes – Never globally uniform. In: Collinson J (ed.) *Correlation in Hydrocarbon Exploration*, pp. 13–19. London: Norwegian Petroleum Society (Graham and Trotman Inc.).
Fletcher BJ, Brentnall SJ, Anderson CW, Berner RA, and Beerling DJ (2008) Atmospheric carbon dioxide linked with Mesozoic and early Cenozoic climate change. *Nature Geoscience* 1: 43–48.
Flögel S, Wallmann K, and Kuhnt W (2011) Cool episodes in the Cretaceous – Exploring the effects of physical forcings on Antarctic snow accumulation. *Earth and Planetary Science Letters* 307: 279–288.
Forster A, Schouten S, Baas M, and Sinninghe Damsté JS (2007) Mid-Cretaceous (Albian–Santonian) sea surface temperature record of the tropical Atlantic Ocean. *Geology* 7: 919–922.
Forster A, Schouten S, Moriya K, Wilson PA, and Sinninghe Damsté JS (2007) Tropical warming and intermittent cooling during the Cenomanian/Turonian oceanic anoxic event 2: Sea surface temperature records from the equatorial Atlantic. *Paleoceanography* 22. http://dx.doi.org/10.1029/2006PA001349.
Frakes LA (1979) *Climates Through Geologic Time*, p. 310. New York: Elsevier.
Frakes LA, Alley NF, and Deynoux M (1995) Early Cretaceous ice rafting and climate Zonation in Australia. *International Geology Review* 37: 567–583.
Frakes LA and Francis JE (1988) A guide to Phanerozoic cold polar climates from high-latitude ice-rafting in the Cretaceous. *Nature* 333: 547–549.
Frakes LA, Francis JE, and Syktus JI (1992) *Climate Modes of the Phanerozoic, p 274*. New York: Cambridge University Press.
Frank TD, Arthur MA, and Dean WE (1999) Diagenesis of lower Cretaceous pelagic carbonates, North Atlantic: Paleoceanographic signals obscured. *Journal of Foraminiferal Research* 29: 340–351.
Franks PJ and Beerling DJ (2009) Maximum leaf conductance driven by CO_2 effects on stomatal size and density over geologic time. *Proceedings of the National Academy of Sciences* 106: 10343–10347.
Freeman KH and Hayes JM (1992) Fractionation of carbon isotopes by phytoplankton and estimates of ancient CO_2 levels. *Global Biogeochemical Cycles* 6: 185–198.
Fricke HC and Wing SL (2004) Oxygen isotope and paleobotanical estimates of temperature and $\delta^{18}O$-latitude gradients over North America during the early Eocene. *American Journal of Science* 304: 612–635.
Friedrich O, Norris RD, and Erbacher J (2012) Evolution of middle to late Cretaceous oceans – A 55 m.y. record of Earth's temperature and carbon cycle. *Geology* 40: 107–110.
Frierson DMW, Lu J, and Chen G (2007) Width of the Hadley cell in simple and comprehensive general circulation models. *Geophysical Research Letters* 34: L18804.
Frijia G and Parente M (2008) Strontium isotope stratigraphy in the upper Cenomanian shallow-water carbonates of the southern Apennines: Short-term perturbations of marine Sr-$^{87}Sr/^{86}Sr$ during the Oceanic Anoxic Event 2. *Palaeogeography, Palaeoclimatology, Palaeoecology* 261: 15–29.
Gale AS, Hardenbol J, Hathaway B, Kennedy WJ, Young JR, and Phansalkar V (2002) Global correlation of Cenomanian (upper Cretaceous) sequences: Evidence for Milankovitch control on sea level. *Geology* 30: 291–294.
Gale AS, Voigt S, Sageman BB, and Kennedy WJ (2008) Eustatic sea-level record for the Cenomanian (late Cretaceous) – Extension to the Western Interior Basin, USA. *Geology* 36: 859–862.
Galeotti S, Krishnan S, Pagani M, et al. (2010) Orbital chronology of early Eocene hyperthermals from the Contessa Road section, central Italy. *Earth and Planetary Science Letters* 290: 192–200.
Galeotti S, Rusciadelli G, Sprovieri M, Lanci L, Gaudio A, and Pekar S (2009) Sea-level control on facies architecture in the Cenomanian–Coniacian Apulian margin (Western Tethys): A record of glacio-eustatic fluctuations during the Cretaceous greenhouse? *Palaeogeography, Palaeoclimatology, Palaeoecology* 276: 196–205.
Gingerich PD, Rose KD, and Krause DW (1980) Early Cenozoic mammalian faunas of the Clark's Fork Basin-Polecat Bench area, northwestern Wyoming. *University of Michigan Papers on Paleontology* 24: 51–68.
Greenwood DR, Basinger JF, and Smith RY (2010) How wet was the Arctic Eocene rain forest? Estimates of precipitation from Paleogene Arctic macrofloras. *Geology* 38: 15–18.
Greenwood DR and Wing SL (1995) Eocene continental climates and latitudinal temperature gradients. *Geology* 23: 1044–1048.
Hague AM, Thomas DJ, Huber M, Korty R, Woodard SC, and Jones LB (2012) Convection of North Pacific deep water during the early Cenozoic. *Geology* 40: 527–530.
Hallam A (1985) A review of Mesozoic climates. *Journal of the Geological Society of London* 142: 433–445.
Haq BU, Hardenbol J, and Vail PR (1987) Chronology of fluctuating sea levels since the Triassic. *Science* 235: 1156–1167.
Haworth M, Hesselbo SP, McElwain JC, Robinson SA, and Brunt JW (2005) Mid-Cretaceous pCO_2 based on stomata of the extinct conifer Pseudofrenelopsis (Cheirolepidiaceae). *Geology* 33: 749–752.
Hay WW (2008) Evolving ideas about the Cretaceous climate and ocean circulation. *Cretaceous Research* 29: 725–753.
Hay WW and Southam JR (1977) Modulation of marine sedimentation by the continental shelves. In: Anderson NR and Malahoff A (eds.) *The Fate of Fossil Fuel CO_2 in the Oceans. Marine Science Series*, vol. 6, pp. 569–604. New York: Plenum Press.
Head JJ, Bloch JI, Hastings AK, et al. (2009) Giant boid snake from the Palaeocene neotropics reveals hotter past equatorial temperatures. *Nature* 457: 715–718.
Held IM and Soden GJ (2006) An assessment of climate feedbacks in coupled ocean–atmosphere models. *Journal of Climate* 19: 3354–3360.
Herman AB and Spicer RA (1996) Paleobotanical evidence for a warm Cretaceous Arctic Ocean. *Nature* 380: 330–333.
Higgins JA and Schrag DP (2006) Beyond methane: Towards a theory for the Paleocene–Eocene thermal maximum. *Earth and Planetary Science Letters* 245: 523–537.
Hollis CJ, Handley L, Crouch EM, et al. (2009) Tropical sea temperatures in the high-latitude South Pacific during the Eocene. *Geology* 37: 99–102.
Hollis CJ, Taylor KWR, Handley L, et al. (2012) Early Paleogene temperature history of the Southwest Pacific Ocean: Reconciling proxies and models. *Earth and Planetary Science Letters* 349–350: 53–56.
Hong SK and Lee YI (2012) Evaluation of atmospheric carbon dioxide concentrations during the Cretaceous. *Earth and Planetary Science Letters* 327–328: 23–28.
Hooker JJ (1996) Mammalian biostratigraphy across the Paleocene–Eocene boundary in the Paris, London and Belgian basins. In: Knox RO, et al. (eds.) *Correlation of the Early Paleogene in Northwest Europe. Geological Society Special Publication*, 101, p. 20. London: Geological Society.
Huber BT (1998) Tropical paradise at the Cretaceous Poles? *Science* 282: 2199–2200.
Huber M (2008) A hotter greenhouse? *Science* 321: 353–354.
Huber M (2009) Snakes tell a torrid tale. *Nature* 457: 669–671.
Huber M and Caballero R (2003) Eocene El Niño: Evidence for robust tropical dynamics in the "hothouse". *Science* 299: 877–881.
Huber BT, Hodell DA, and Hamilton CP (1995) Middle–late Cretaceous climate of the southern high latitudes: Stable isotopic evidence for minimal equator-to-pole thermal gradients. *Geological Society of America Bulletin* 107: 1164–1191.
Huber BT, Leckie RM, Norris RD, Bralower TJ, and CoBabe E (1999) Foraminiferal assemblage and stable isotopic change across the Cenomanian–Turonian boundary in the subtropical North Atlantic. *Journal of Foraminiferal Research* 29: 392–417.
Huber BT, Norris RD, and MacLeod KG (2002) Deep-sea paleotemperature record of extreme warmth during the Cretaceous. *Geology* 30: 123–126.
Huber M and Sloan LC (1999) Warm climate transitions: A general circulation modeling study of the late Paleocene thermal maximum (56 Ma). *Journal of Geophysical Research* 104: 16633–16655.

Huber M and Sloan LC (2000) Climatic responses to tropical sea surface temperature changes on a "greenhouse" Earth. *Paleoceanography* 15: 443–450.
Huber M and Sloan LC (2001) Heat transport, deep waters, and thermal gradients: Coupled simulation of an Eocene greenhouse climate. *Geophysical Research Letters* 28: 3481–3484.
Huber M, Sloan LC, and Shellito C (2003) Early Paleogene oceans and climate: A fully coupled modelling approach using NCAR's CSM. In: Wing SL, Gingerich PD, Schmitz B, and Thomas E (eds.) *Causes and Consequences of Globally Warm Climates in the Early Paleogene*. *Geologogical Society of America Special Paper* 369, pp. 25–47. Boulder, CO: Geological Society of America.
Hutchinson JH (1982) Turtle, crocodilian, and champsosaur diversity changes in the Cenozoic of the north-central region of western United States. *Palaeogeography, Palaeoclimatology, Palaeoecology* 37: 149–164.
Ingalls AE, Shah SR, Hansman RL, et al. (2006) Quantifying archaeal community autotrophy in the mesopelagic ocean using natural radiocarbon. *Proceeding of the National Academy of Sciences of the United States of America* 103: 6442–6447.
Jenkyns HC, Forster A, Schouten S, and Sinninghe Damsté JS (2004) High temperatures in the late Cretaceous Arctic Ocean. *Nature* 432: 888–892.
Jenkyns HC, Schouten-Huibers L, Schouten S, and Sinninghe Damsté JS (2012) Warm middle Jurassic–early Cretaceous high-latitude sea-surface temperatures from the Southern Ocean. *Climates of the Past* 8: 215–226.
Joachimski MM and Buggisch W (1993) Anoxic events in the late Frasnian – Causes of the Frasnian–Famennian faunal crisis? *Geology* 21: 675–678.
Jones TD, Ridgwell A, Lunt DJ, Maslin MA, Schmidt DN, and Valdes PJ (2010) A Paleogene perspective on climate sensitivity and methane hydrate instability. *Philosophical Transactions of the Royal Society A* 368: 2395–2415.
Jordan GJ (2011) A critical framework for the assessment of biological palaeoproxies: Predicting past climate and levels of atmospheric CO_2 from fossil leaves. *New Phytologist* 192: 29–44.
Kelly DC, Bralower TJ, and Zachos JC (2001) On the demise of the early Paleogene Morozovella velascoensis lineage: Terminal progenesis in the planktonic foraminifera? *Palaios* 16: 507–523.
Kennett JP and Stott LD (1990) Proteus and Proto-Oceanus: Paleogene oceans as revealed from Antarctic stable isotopic results. In: Barker PF and Kennett JP, et al. (eds.) *Scientific Results, Proceedings of the Ocean Drilling Program, Leg 113: College Station, Texas, Ocean Drilling Program*, pp. 865–880.
Kennett JP and Stott LD (1991) Abrupt deep-sea warming, palaeoceanographic changes and benthic extinctions at the end of the Paleocene. *Nature* 353: 225–229.
Kennett JP and Stott LD (1995) Terminal Paleocene mass extinction in the deep sea. In: *Effects of Past Global Change on Life*, p. 250. Washington, DC: National Academy Press.
Kerr AC (1998) Oceanic plateau formation: A cause of mass extinction and black shale deposition around the Cenomanian–Turonian boundary. *Journal of the Geological Society of London* 155: 619–626.
Kerr AC (2005) Oceanic LIPs: The kiss of death. *Elements* 1: 289–292.
Kim J-H, Schouten S, Hopmans EC, Donner B, and Sinninghe Damsté JS (2008) Global sediment core-top calibration of the TEX_{86} paleothermometer in the ocean. *Geochimica et Cosmochimica Acta* 72: 1154–1173.
Kim J-H, van der Meer J, Schouten S, et al. (2010) New indices and calibrations derived from the distribution crenarchaeal isoprenoid tetraether lipids: Implications for past sea surface temperature reconstructions. *Geochimica et Cosmochimica Acta* 74: 4639–4654.
Kirk-Davidoff DB and Lamarque J-F (2008) Maintenance of polar stratospheric clouds in a moist stratosphere. *Climate of the Past* 4: 69–78.
Kirk-Davidoff DB, Schrag D, and Anderson J (2002) On the feedback of stratospheric clouds on polar climate. *Geophysical Research Letters* 29. http://dx.doi.org/10.1029/2002GL014659.
Knutti R and Hegerl GC (2008) The equilibrium sensitivity of the Earth's temperature to radiation changes. *Nature Geoscience* 1: 735–743.
Koch JT and Brenner RL (2009) Evidence for glacioeustatic control of large, rapid sea-level fluctuations during the Albian-Cenomanian: Dakota formation, eastern margin of western interior seaway, USA. *Cretaceous Research* 30: 411–423.
Kominz MA, Browning JV, Miller KG, Sugarman PJ, Misintzeva S, and Scotese CR (2008) Late Cretaceous to Miocene sea-level estimates from the New Jersey and Delaware coastal plain coreholes: An error analysis. *Basin Research* 20: 211–226.
Kowalski EA and Dilcher DL (2002) Warmer temperatures for terrestrial ecosystems. *Proceedings of the National Academy of Sciences* 100: 167–170.
Kozdon R, Kelly DC, Kita NT, Fournelle JH, and Valley JW (2011) Planktonic foraminiferal oxygen isotope analysis by ion microprobe technique suggests warm tropical sea surface temperatures during the early Paleogene. *Paleoceanography* 26. http://dx.doi.org/10.1029/2010PA002056.
Kraus MJ and Riggins S (2007) Transient drying during the Paleocene–Eocene Thermal Maximum (PETM): Analysis of paleosols in the Bighorn Basin, Wyoming. *Palaeogeography, Palaeoclimatology, Palaeoecology* 245: 444–461.
Kuiper KF, Deino A, Hilgen FJ, Krijgsman W, Renne PR, and Wijbrans JR (2008) Synchronizing rock clocks of earth history. *Science* 320: 500–504.
Kump LR and Pollard D (2008) Amplification of Cretaceous warmth by biological cloud feedbacks. *Science* 320: 195.
Kuroda J, Ogawa NO, Tanimizu M, et al. (2007) Contemporaneous massive subaerial volcanism and late Cretaceous oceanic anoxic event 2. *Earth and Planetary Science Letters* 256: 211–223.
Kurtz AC, Kump LR, Arthur MA, Zachos JC, and Paytan A (2003) Early Cenozoic decoupling of the global carbon and sulfur cycles. *Paleoceanography* 18. http://dx.doi.org/10.1029/2003PA000908.
Lambeck K and Chappell J (2001) Sea level change through the last glacial cycle. *Science* 292: 679–686.
Larson RL (1991a) Geological consequences of superplumes. *Geology* 19: 963–966.
Larson RL (1991b) Latest pulse of Earth: Evidence for a mid-Cretaceous superplume. *Geology* 19: 547–550.
Lawrence KT, Sloan LC, and Sewall JO (2003) Terrestrial climatic response to precessional orbital forcing in the Eocene. In: Wing S, Gingerich P, Schmitz B, and Thomas E (eds.) *Causes and Consequences of Globally Warm Climates in the Early Paleogene*. vol. 369, *Geological Society of America Special Paper, Boulder, Colorado*, pp. 65–77. Boulder, CO: Geological Society of America.
Lear C, Bailey T, Pearson P, Coxall H, and Rosenthal Y (2008) Cooling and ice growth across the Eocene–Oligocene transition. *Geology* 36: 251–254.
Lear CH, Elderfield H, and Wilson PA (2000) Cenozoic deep-sea temperatures and global ice volumes from Mg/Ca in benthic foraminiferal calcite. *Science* 287: 269–272.
Leckie RM, Bralower T, and Cashman R (2002) Oceanic Anoxic Events and plankton evolution: Biotic response to tectonic forcing during the mid-Cretaceous. *Paleoceanography* 17. http://dx.doi.org/10.1029/2001PA000623.
Lindzen RS (1993) Paleoclimate sensitivity. *Nature* 363: 25–26.
Lindzen RS (1994) Climate dynamics and global change. *Annual Review of Fluid Mechanics* 26: 353–378.
Lindzen RS (1997) Can increasing atmospheric CO_2 affect global climate? *Proceedings of the National Academy of Science* 94: 8335–8342.
Lindzen RS and Farrell B (1977) Some realistic modifications of simple climate models. *Journal of the Atmospheric Sciences* 34: 1487–1501.
Littler K, Robinson SA, Bown PR, Nederbragt AJ, and Pancost RD (2011) High sea-surface temperatures during the early Cretaceous Epoch. *Nature Geoscience* 4: 169–172.
Liu Z, Pagani M, Zinniker D, et al. (2009) Global cooling during the Eocene–Oligocene climate transition. *Science* 323: 1187–1190.
Lourens L, Sluijs A, Kroon D, et al. (2005) Astronomical pacing of late Palaeocene to early Eocene hyperthermal events. *Nature* 435: 1083–1087.
Lowenstam HA and Epstein S (1954) Paleotemperatures of the post-Aptian Cretaceous as determined by the oxygen isotope method. *Journal of Geology* 62: 207–248.
Lowenstein TK and Demicco RV (2006) Elevated Eocene atmospheric CO_2 and its subsequent decline. *Science* 313: 1928.
Lu J, Vecchi GA, and Reichler T (2007) Expansion of the Hadley cell under global warming. *Geophysical Research Letters* 34: L06805.
Lunt DJ, Jones TD, Heinemann M, et al. (2012) A model-data comparison for a multi-model ensemble of early Eocene atmosphere–ocean simulations: EoMIP. *Climates of the Past* 8: 1229–1273.
Lyle M (1997) Could early Cenozoic thermohaline circulation have warmed the poles? *Paleoceanography* 12: 161–167.
Maas MC, Anthony MRL, Gingerich PD, Gunnell GF, and Krause DW (1995) Mammalian generic diversity and turnover in the late Paleocene and early Eocene of the Bighorn and Crazy Mountains Basins Wyoming and Montana (USA). *Palaeogeography, Palaeoclimatology, Palaeoecology* 115: 181–207.
Markwick PJ (1998) Fossil crocodilians as indicators of late Cretaceous and Cenozoic climates: Implications for using palaeontological data in reconstructing palaeoclimate. *Palaeogeography, Palaeoclimatology, Palaeoecology* 137: 205–271.
Markwick PJ (2007) The palaeogeographic and palaeoclimatic significance of climate proxies for data-model comparisons. In: Williams M, Haywood AM, Gregory FJ, and Schmidt DN (eds.) *Deep-Time Perspectives on Climate Change: Marrying the Signal from Computer Models and Biological Proxies*, The Micropalaeontological Society, Special Publications, pp. 251–312. London: The Geological Society.
Meyer KJ and Kump LR (2008) Oceanic Euxinia in Earth history: Causes and consequences. *Annual Reviews of Earth and Planetary Sciences* 36: 251–288.

Meyers SR, Siewert SE, Singer BS, et al. (2012) Intercalibration of radioisotopic and astrochronologic time scales for the Cenomanian/Turonian boundary interval, Western Interior Basin, USA. *Geology* 40: 7–10.

Miall AD (1992) Exxon global cycle chart: An event for every occasion? *Geology* 20: 787–790.

Miller KG (2009) Broken greenhouse windows. *Nature Geoscience* 2: 465–466.

Miller KG, Janacek TR, Katz ME, and Keil DJ (1987) Abyssal circulation and benthic foraminiferal changes near the Paleocene/Eocene Boundary. *Paleoceanography* 2: 741–761.

Miller KG, Kominz MA, Browning JV, et al. (2005) The Phanerozoic record of sea-level change. *Science* 310: 1293–1298.

Miller KG, Mountain GS, Wright JD, and Browning JV (2011) A 180-million year record of sea level and ice volume variations from continental margin and deep-sea isotopic records. *Oceanography* 24: 40–53.

Miller KG, Wright JD, and Browning JV (2005) Visions of ice sheets in a greenhouse world. *Marine Geology* 217: 215–231.

Mitrovica JX, Gomez N, Morrow E, Hay C, Latychev K, and Tamisiea ME (2011) On the robustness of predictions of sea level fingerprints. *Geophysical Journal International* 187: 729–742.

Mitrovica JX, Tamisiea ME, Davis JL, and Milne GA (2001) Recent mass balance of polar ice sheets inferred from patterns of global sea-level change. *Nature* 409: 1026–1029.

Montañez IP (2013) Modern soil system constraints on reconstructing deep-time atmospheric CO_2. *Geochimica et Cosmochimica Acta* 101: 57–75.

Montañez IP and Poulsen CJ (2013) The late Paleozoic Ice Age: An evolving icehouse paradigm. *Annual Reviews in Earth and Planetary Sciences* 41: 629–656.

Montañez IP, Tabor NJ, Niemeier D, et al. (2007) CO_2-forced climate and vegetation instability during late Paleozoic deglaciation. *Science* 315: 87–91.

Moran K, et al. (2006) The Cenozoic palaeoenvironment of the Arctic Ocean. *Nature* 441: 601–605.

Moriya K, Wilson PA, Friedrich O, Erbacher J, and Kawahata H (2007) Testing for ice sheets during the mid-Cretaceous greenhouse using glassy foraminiferal calcite from the mid-Cenomanian tropics on Demerara Rise. *Geology* 7: 615–618.

Morner N-A (1976) Eustasy and geoid changes. *Journal of Geology* 84: 123–151.

Morrill C, Small EE, and Sloan LC (2001) Modeling orbital forcing of lake level change: Lake Gosiute (Eocene), North America. *Global and Planetary Change* 29: 57–76.

Mort HP, Adatte T, Follmi KB, et al. (2007) Phosphorus and the roles of productivity and nutrient recycling during oceanic anoxic event 2. *Geology* 35: 483–486.

Najjar RG, Nong GT, Seidov D, and Peterson WH (2002) Modeling geographic impacts on early Eocene ocean temperature. *Geophysical Research Letters* 29. http://dx.doi.org/10.1029/2001GL014-438.

Nicol GW and Schleper C (2006) Ammonia-oxidising Crenarchaeota: Important players in the nitrogen cycle? *Trends in Microbiology* 14: 207–212.

Noone D (2008) The influence of midlatitude and tropical overturning circulation on the isotopic composition of atmospheric water vapor and Antarctic precipitation. *Journal of Geophysical Research* 113: D04102.

Norris RD, Bice KL, Magno EA, and Wilson PA (2002) Jiggling the tropical thermostat in the Cretaceous hothouse. *Geology* 30: 299–302.

Norris RD and Wilson PA (1998) Low-latitude sea-surface temperatures for the mid-Cretaceous and the evolution of planktic foraminifera. *Geology* 26: 823–826.

Olivarez Lyle A and Lyle MW (2006) Missing organic carbon in Eocene marine sediments: Is metabolism the biological feedback that maintains end-member climates? *Paleoceanography* 21: PA2007.

Otto-Bliesner BL, Brady EC, and Shields C (2002) Center for Atmospheric Research Climate System Model. *Journal of Geophysical Research* 107. http://dx.doi.org/10.1029/2001JD000821.

Otto-Bliesner BL and Upchurch GR (1997) Vegetation-induced warming of high-latitude regions during the late Cretaceous period. *Nature* 385: 804–807.

Pagani M, Caldeira K, Archer D, and Zachos JC (2006) An ancient carbon mystery. *Science* 314: 1556–1557.

Pagani M, Liu Z, LaRiviera J, and Ravelo AC (2009) High climate sensitivity to atmospheric carbon dioxide for the past 5 million years. *Nature Geoscience* 3: 27–30.

Pagani M, Zachos J, Freeman KH, Bohaty S, and Tipple B (2005) Marked change in atmospheric carbon dioxide concentrations during the Oligocene. *Science* 309: 600–603.

Pagani M, Pedentchouk N, Huber M, et al. (2006b) Arctic hydrology during global warming at the Palaeocene–Eocene thermal maximum. *Nature* 442: 671–675.

Pälike H, Norris RD, Herrle JO, et al. (2006) The heartbeat of the Oligocene climate system. *Science* 314: 1894–1898.

Panchuk K, Ridgwell A, and Kump L (2008) Sedimentary response to Paleocene–Eocene thermal maximum carbon release: A model data comparison. *Geology* 36: 315–318.

Park J and Royer DL (2011) Geological constraints on the glacial amplification of Phanerozoic climate sensitivity. *American Journal of Science* 311. http://dx.doi.org/10.2475/01.2011.01.

Parrish JT and Spicer RA (1988) Late Cretaceous terrestrial vegetation: A near-polar temperature curve. *Geology* 16: 22–25.

Pavlov AA, Kastings JF, Brown LL, Rages KA, and Freedman R (2000) Greenhouse warming by CH_4 in the atmosphere of early Earth. *Journal of Geophysical Research* 105: 11,981–11,990.

Pearson PN, Ditchfield PW, Singano J, et al. (2001) Warm tropical sea surface temperatures in the late Cretaceous and Eocene epochs. *Nature* 413: 481–487.

Pearson PN and Palmer MR (2000) Atmospheric carbon dioxide concentrations over the past 60 million years. *Nature* 206: 695–699.

Pearson P, van Dongen BE, Nicholas CJ, et al. (2007) Stable warm tropical climate through the Eocene Epoch. *Geology* 35: 211–214.

Peters RB and Sloan LC (2000) High concentrations of greenhouse gases and polar stratospheric clouds: A possible solution to high-latitude faunal migration at the latest Paleocene thermal maximum. *Geology* 28: 979–982.

Pettijohn F (1957) *Sedimentary Rocks*, p. 718. New York: Harper.

Pierrehumbert RT (1995) Thermostats, radiator fins, and the local runaway greenhouse. *Journal of Atmospheric Sciences* 52: 1784–1806.

Pierrehumbert RT (1998) Lateral mixing as a source of subtropical water vapor. *Geophysical Research Letters* 25: 151–154.

Pierrehumbert RT (2002) The hydrologic cycle in deep time climate problems. *Nature* 419: 191–198.

Pirrie D and Marshall JD (1990) High paleolatitude late Cretaceous paleotemperatures: New data from James Ross Island, Antarctica. *Geology* 18: 31–34.

Plass GN (1956) The carbon dioxide theory of climatic change. *Tellus* 8: 140–154.

Pollard D and DeConto RM (2005) Hysteresis in Cenozoic Antarctic ice-sheet variations. *Global and Planetary Change* 45: 9–21.

Poole I, Cantrill D, and Utescher T (2005) A multi-proxy approach to determine Antarctic terrestrial palaeoclimate during the late Cretaceous and early Tertiary. *Palaeogeography, Palaeoclimatology, Palaeoecology* 222: 95–121.

Popp BN, Takigiku R, Hayes JM, Louda JW, and Baker EW (1989) The post-Paleozoic chronology and mechanism of ^{13}C depletion in primary marine organic matter. *American Journal of Science* 289: 436–454.

Poulsen CJ, Barren EJ, Peterson WH, and Wilson PA (1999) A reinterpretation of mid-Cretaceous shallow marine temperatures through model-data comparison. *Paleoceanography* 14: 679–697.

Poulsen CJ, Barron EJ, Arthur MA, and Peterson WH (2001) Response of the mid-Cretaceous global oceanic circulation to tectonic and CO_2 forcings. *Paleoceanography* 16: 576–592.

Poulsen CJ, Flemings PB, Robinson RAJ, and Metzger JM (1998) Three-dimensional stratigraphic evolution of the Miocene Baltimore Canyon region: Implications for eustatic interpretations and the systems tract model. *GSA Bulletin* 110: 1105–1122.

Poulsen CJ, Gendaszek AS, and Jacob RL (2003) Did the rifting of the Atlantic Ocean cause the Cretaceous thermal maximum. *Geology* 31: 115–118.

Prahl FG, Wolfe GV, and Sparrow MA (2003) Physiological impacts on alkenone paleothermometry. *Paleoceanography* 18. http://dx.doi.org/10.1029/2002PA000803.

Pratt LM (1985) Isotopic studies of organic matter and carbonate in rocks of the Greenhorn Marine Cycle. In: Pratt LM, Kauffman EG, and Zelt FB (eds.) *Fine-Grained Deposits and Biofacies of the Cretaceous Western Interior Seaway: Evidence of Cyclic Sedimentary Processes: SEPM, Field Trip Guidebook No. 4*, pp. 38–48. Tulsa: SEPM.

Price GD (1999) The evidence and implications of polar ice during the Mesozoic. *Earth-Science Reviews* 48: 183–210.

Price GD and Nunn EV (2010) Valanginian isotope variation in glendonites and belemnites from Arctic Svalbard: Transient glacial temperatures during the Cretaceous greenhouse. *Geology* 38: 251–254.

Pross J, Contreras L, Bijl PK, et al. (2012) Persistent near-tropical warmth on the Antarctic continent during the early Eocene epoch. *Nature* 488: 73–77.

Pucéat E, Lécuyer C, Donnadieu Y, et al. (2007) Fish tooth $\delta^{18}O$ revising late Cretaceous meridional upper ocean water temperature gradients. *Geology* 35: 107–110.

Quan C, Sun C, Sun Y, and Sun G (2009) High resolution estimates of paleo-CO_2 levels through the Campanian (late Cretaceous) based on Ginkgo cuticles. *Cretaceous Research* 30: 424–428.

Raymo ME, Mitrovica JX, O'Leary MJ, DeConto RM, and Hearty PJ (2011) Departures from eustasy in Pliocene sea-level records. *Nature Geoscience* 4: 328–332.

Retallack GJ (2001) A 300-million-year record of atmospheric carbon dioxide from fossil plant cuticles. *Nature* 411: 287–290.

Rind D and Chandler M (1991) Increased ocean heat transports and warmer climate. *Journal of Geophysical Research* 96: 7437–7461.

Roberts CD, LeGrande AN, and Tripati AK (2009) Climate sensitivity to Arctic seaway restriction during the early Paleogene. *Earth and Planetary Science Letters* 286: 576–585.

Robinson SA and Vance D (2012) Widespread and synchronous change in deep-ocean circulation in the North and South Atlantic during the late Cretaceous. *Paleoceanography* 27: PA1102.

Roche DM, Donnadieu Y, Pucéat E, and Paillard D (2006) Effect of changes in $d^{18}O$ content of the surface ocean on estimated sea surface temperatures in past warm climate. *Paleoceanography* 21: PA2023.

Roe GH and Baker MB (2007) Why is climate sensitivity so unpredictable? *Science* 318: 629–632.

Royer DL (2003) Estimating latest Cretaceous and Tertiary atmospheric CO_2 from stomatal indices. In: Wing SL, Gingerich PD, Schmitz B, and Thomas E (eds.) *Causes and Consequences of Globally Warm Climates in the Early Paleogene: Boulder, Colorado, GSA Special Paper* 369, pp. 79–93. Boulder, CO: Geological Society of America.

Royer DL (2006) CO_2-forced climate thresholds during the Phanerozoic. *Geochimica et Cosmochimica Acta* 70: 5665–5675.

Sagan C and Mullen G (1972) Earth and Mars: Evolution of atmospheres and surface temperatures. *Science* 177: 52–56.

Saltzman ES and Barron EJ (1982) Circulation in the late Cretaceous: Oxygen isotope paleotemperatures from *Inoceramus* remains in DSDP cores. *Palaeogeography, Palaeoclimatology, Palaeoecology* 40: 167–181.

Savin SM (1977) The history of the Earth's surface temperature during the past 100 million years. *Annual Reviews of Earth and Planetary Sciences* 5: 319–355.

Savin SM, Douglas RG, and Stehli FG (1975) Tertiary marine paleotemperatures. *Geological Society of America Bulletin* 86: 1499–1510.

Schlanger SO and Jenkyns HC (1976) Cretaceous anoxic events: Causes and consequences. *Geologie En Mijnbouw* 55: 179–184.

Schmidt GA and Mysak LA (1996) Can increased poleward oceanic heat flux explain the warm Cretaceous climate? *Paleoceanography* 11: 579–593. http://dx.doi.org/10.1029/96PA01851.

Schouten S, Hopmans EC, Forster A, van Breugel Y, Kuypers MMM, and Sinninghe Damsté JS (2003) Extremely high sea-surface temperatures at low latitudes during the middle Cretaceous as revealed by archaeal membrane lipids. *Geology* 31: 1069–1072.

Schouten S, Hopmans EC, Schefuß E, and Sinninghe Damsté JS (2002) Distributional variations in marine crenarchaeotal membrane lipids: A new organic proxy for reconstructing ancient sea water temperatures? *Earth and Planetary Science Letters* 204: 265–274.

Schrag DP (1999) Effects of diagenesis on the isotopic record of late Paleogene tropical sea surface temperatures. *Chemical Geology* 161: 215–224.

Schuur EAG, Bockheim J, Canadell JG, et al. (2008) Vulnerability of permafrost carbon to climate change: Implications for the global carbon cycle. *Bioscience* 58: 701–714.

Schuur EAG, Vogel JG, Crummer KG, Lee H, Sickman JO, and Osterkanp TE (2009) The effect of permafrost thaw on old carbon release and net carbon exchange from tundra. *Nature* 459: 556–559.

Seager R, Ting M, Held I, et al. (2007) Model projections of an imminent transition to a more arid climate in the southwestern North America. *Science* 316: 1181–1184.

Sellwood BW, Price GD, and Valdes PJ (1994) Cooler temperatures of the Cretaceous. *Nature* 370: 453–455.

Sewall JO, Huber M, and Sloan LC (2004) A method for using a fully coupled climate system model to generate detailed surface boundary conditions for paleoclimate modeling investigations: An early Paleogene example. *Global and Planetary Change* 43: 173–182.

Sewall JO and Sloan LC (2001) Equable Paleogene climates: The result of a stable, positive Arctic oscillation? *Geophysical Research Letters* 28: 3693–3695.

Sewall JO and Sloan LC (2004) Less ice, less tilt, less chill: The influence of a seasonally ice-free Arctic Ocean and changing obliquity on early Paleogene climate. *Geology* 32: 477–480.

Sewall J and Sloan LC (2006) Come a little bit closer: A high-resolution climate study of the early Paleogene Laramide foreland. *Geology* 34: 81–84.

Sewall JO, Sloan LC, Huber M, and Wing S (2000) Climate sensitivity to changes in land surface characteristics. *Global and Planetary Change* 26: 445–465.

Sexton PF, Wilson PA, and Pearson PN (2006) Microstructural and geochemical perspectives on planktic foraminiferal preservation: "Glassy" versus "frosty". *Geochemistry, Geophysics, Geosystems* 7. http://dx.doi.org/10.1029/2006GC001291.

Shackleton NJ and Kennett JP (1975) Paleotemperature history of the Cenozoic and the initiation of Antarctic glaciation: Oxygen and carbon isotope analyses in DSDP sites 277, 279, and 281. *Deep Sea Drilling Program Initial Reports* 29: 743–755.

Shah SR, Mollenhauer G, Ohkouchi N, Eglinton TI, and Pearson A (2008) Origins of archaeal tetraether lipids in sediments: Insights from radiocarbon analysis. *Geochimica et Cosmochimica Acta* 72: 4577–4594.

Sheldon ND and Retallack GJ (2004) Regional paleoprecipitation from the late Eocene and Oligocene of North America. *Journal of Geology* 112: 487–494.

Shellito CJ, Lamarque J-F, and Sloan LC (2009) Early Eocene Arctic climate sensitivity to pCO_2 and basin geography. *Geophysical Research Letters* 36: L09707.

Shellito C and Sloan LC (2006a) Reconstructing a lost Eocene Paradise. Part I. Simulating the change in global floral distribution at the initial Eocene thermal maximum. *Global and Planetary Change* 50: 1–17.

Shellito C and Sloan LC (2006b) Reconstructing a lost Eocene Paradise, Part II: On the utility of dynamic global vegetation models in pre-quaternary climate studies. *Global and Planetary Change* 50: 18–32.

Shellito CJ, Sloan LC, and Huber M (2003) Climate model sensitivity to atmospheric CO_2 levels in the early–middle Paleogene. *Palaeogeography, Palaeoclimatology, Palaeoecology* 193: 113–123.

Sickel WAV, Kominz MA, Miller KG, and Browning JV (2004) Late Cretaceous and Cenozoic sea-level estimates: Backstripping analysis of borehole data, onshore New Jersey. *Basin Research* 16: 451–465.

Sijp WP, England MH, and Huber M (2011) Effect of the deepening of the Tasman Gateway on the global ocean. *Paleoceanography* 26: PA4207.

Sinton CW and Duncan RA (1997) Potential links between ocean plateau volcanism and global ocean anoxia at the Cenomanian–Turonian boundary. *Economic Geology* 92: 836–842.

Sloan LC (1994) Equable climates during the early Eocene: Significance of regional paleogeography for North American climate. *Geology* 22: 881–884.

Sloan LC and Barron EJ (1990) "Equable" climates during Earth history? *Geology* 18: 89–492.

Sloan LC, Huber M, Crowley TJ, Sewall JO, and Baum SK (2001) Effect of sea surface temperature configuration on model simulations of "equable" climate in the early Eocene. *Palaeogeography, Palaeoclimatology, Palaeoecology* 167: 321–335.

Sloan LC, Huber M, and Ewing A (1999) Polar stratospheric cloud forcing in a greenhouse world. In: Abrantes F and Mix AC (eds.) *Reconstructing Ocean History: A Window into the Future*, pp. 273–293. New York: Kluwer Academic.

Sloan LC and Morrill C (1998) Orbital forcing and Eocene continental temperatures. *Palaeogeography, Palaeoclimatology, Palaeoecology* 144: 21–35.

Sloan LC and Pollard D (1998) Polar stratospheric clouds: A high-latitude warming mechanism in an ancient greenhouse world. *Geophysical Research Letters* 25: 3517–3520.

Sloan LC and Rea DK (1996) Atmospheric carbon dioxide and early Eocene climate: A general circulation modeling sensitivity study. *Palaeogeography, Palaeoclimatology, Palaeoecology* 119: 275–292.

Sloan LC, Walker JCG, and Moore TC (1995) Possible role of oceanic heat-transport in early Eocene climate. *Paleoceanography* 10: 347–356.

Sloan LC, Walker J, Moore TC, Rea D, and Zachos JC (1992) Possible methane-induced polar warming in the early Eocene. *Nature* 357: 320–322.

Sluijs A, Brinkhuis H, Schouten S, et al. (2007) Environmental precursors to rapid light carbon injection at the Palaeocene/Eocene boundary. *Nature* 450: 1218–1221.

Sluijs A, Schouten S, Donders TH, et al. (2009) Warm and wet conditions in the Arctic region during Eocene thermal maximum 2. *Nature Geoscience* 2: 777–780.

Sluijs A, Schouten S, Pagani M, et al. (2006) Subtropical Arctic Ocean conditions during the Palaeocene Eocene thermal maximum. *Nature* 441: 610–613.

Speelman EN, Sewall JO, Noone D, et al. (2010) Modeling the influence of a reduced equator-to-pole sea surface temperature gradient on the distribution of water isotopes in the Eocene. *Earth and Planetary Science Letters* 298: 57–65.

Speelman EN, van Kempen MML, Barke J, et al. (2009) The Eocene Arctic Azolla bloom: Environmental conditions, productivity and carbon drawdown. *Geobiology* 7: 155–170.

Speijer RP and Morsi A-M (2002) Ostracode turnover and sea-level changes associated with the Paleocene–Eocene thermal maximum. *Geology* 30: 23–26.

Spero HJ, Bijma J, Lea DW, and Bemis BE (1997) Effect of seawater carbonate concentration on foraminiferal carbon and oxygen isotopes. *Nature* 390: 497–500.

Spicer RA, Ahlberg A, Herman AB, Kelley SP, Raikevich MI, and Rees PM (2002) Palaeoenvironment and ecology of the middle Cretaceous Grebenka flora of northeastern Asia. *Palaeogeography, Palaeoclimatology, Palaeoecology* 184: 65–105.

Spicer RA, Ahlberg A, Herman AB, et al. (2008) The late Cretaceous continental interior of Siberia: A challenge for climate models. *Earth and Planetary Science Letters* 267: 228–235.

Spicer RA and Parrish JT (1986) Paleobotanical evidence for cool north polar climates in middle Cretaceous (Albian-Cenomanian) time. *Geology* 14: 703–706.

Spicer RA and Parrish JT (1990) Late Cretaceous–early Tertiary palaeoclimates of northern high latitudes: A quantitative view. *Journal of the Geological Society of London* 147: 329–341.
Spielhagen RF and Tripati A (2009) Evidence from Svalbard for near-freezing temperatures and climate oscillations in the Arctic during the Paleocene and Eocene. *Palaeogeography, Palaeoclimatology, Palaeoecology* 278: 48–56.
Spofforth DJA, Agnini C, Pälike H, et al. (2010) Organic carbon burial following the middle Eocene climatic optimum in the central western Tethys. *Paleoceanography* 25: PA3210.
Stap L, Lourens LJ, Thomas E, Sluijs A, Bohaty S, and Zachos JC (2010) High-resolution deep-sea carbon and oxygen isotope records of Eocene thermal maximum 2 and H2. *Geology* 38: 607–610.
Stein R, Boucsein B, and Meyer H (2006) Anoxia and high primary production in the Paleogene central Arctic Ocean: First detailed records from Lomonosov Ridge. *Geophysical Research Letters* 33: L18606.
Steuber T, Rauch M, Masse J-P, Graaf J, and Malkoč M (2005) Low-latitude seasonality of Cretaceous temperatures in warm and cold episodes. *Nature* 437: 1431–1444.
Stoll HM and Schrag DP (1996) Evidence of glacial control of rapid sea level changes in early Cretaceous. *Science* 272: 1771–1774.
Stoll HM and Schrag DP (2000) High-resolution stable isotope records from the upper Cretaceous rocks of Italy and Spain: Glacial episodes in a greenhouse planet? *Geological Society of America Bulletin* 112: 308–319.
Strøm KM (1936) Land-locked waters. *Det. Norske Videnskaps-Akademi I Oslo, Nat. Naturv. Lasse* 7: 70–81.
Sun D and Lindzen RS (1993) Water vapor feedback and the ice age snowline record. *Annales Geophysicae* 11: 204–215.
Tajika E (1999) Carbon cycle and climate change during the Cretaceous inferred from a biogeochemical carbon cycle model. *The Island Arc* 8: 293–303.
Tarduno JA, Brinkman DB, Renne PR, Cottrell RD, Scher H, and Castillo P (1998) Evidence for extreme climatic warmth from late Cretaceous arctic vertebrates. *Science* 282: 2241–2243.
Thomas E (2007) Cenozoic mass extinctions in the deep sea: What perturbs the largest habitat on Earth? In: Monechi S, Coccioni R, and Rampino MR (eds.) *Large Ecosystem Perturbations: Causes and Consequences. Geological Society of America Special Paper 424*, pp. 1–23. Geological Society of America.
Thomas E and Shackleton NJ (1996) The Paleocene–Eocene benthic foraminiferal extinction and stable isotope anomalies. In: Knox RWOB, Corfield RM, and Dunay RE (eds.) *Correlation of the Early Paleogene in Northwest Europe*, Geological Society Special Publication, pp. 401–441. London: Geological Society.
Thomas E and Zachos JC (2000) Was the late Paleocene thermal maximum a unique event? *GFF* 122: 169–170.
Thompson SL and Barron EJ (1981) Comparison of Cretaceous and present Earth albedos: Implications for the causes of paleoclimates. *Journal of Geology* 89: 143–167.
Thrasher BL and Sloan LC (2009) Carbon dioxide and the early Eocene climate of western North America. *Geology* 37: 807–810.
Tindall J, Flecker R, Valdes P, Schmidt DN, Markwick P, and Harris J (2010) Modeling the oxygen isotope distribution of ancient seawater using a coupled ocean–atmosphere GCM: Implications for reconstructing early Eocene climate. *Earth and Planetary Science Letters* 292: 265–273.
Tripati AK, Delaney ML, Zachos JC, Anderson LD, Kelly DC, and Harry E (2003) Tropical sea-surface temperature reconstruction for the early Paleogene using Mg/Ca ratios of planktonic foraminifera. *Paleoceanography* 18. http://dx.doi.org/10.1029/2003PA000937.
Tripati AK and Elderfield H (2004) Abrupt hydrographic changes in the equatorial Pacific and subtropical Atlantic from foraminiferal Mg/Ca indicate greenhouse origin for the thermal maximum at the Paleocene–Eocene boundary. *Geochemistry, Geophysics, Geosystems* 5. http://dx.doi.org/10.1029/2003GC000631.
Turgeon SC and Creaser RA (2008) Cretaceous oceanic anoxic event 2 triggered by a massive magmatic episode. *Nature* 454: 323–326.
Turich C, Freeman KH, Bruns MA, Conte M, Jones AD, and Wakeham SG (2007) Lipids of marine Archaea: Patterns and provenance in the water-column and sediments. *Geochimica et Cosmochimica Acta* 71: 3272–3291.
Ufnar DF, Gonzalez LA, Ludvigson GA, Brenner RL, and Witzke BJ (2004) Evidence for increased latent heat transport during the Cretaceous (Albian) greenhouse warming. *Geology* 32: 1049–1052.
Uhl D, Klotz S, Traiser C, et al. (2007a) Paleotemperatures from fossil leaves – A European perspective. *Palaeogeography, Palaeoclimatology, Palaeoecology* 248: 24–31.
Uhl D, Traiser C, Griesser U, and Denk T (2007b) Fossil leaves as palaeoclimate proxies in the Palaeogene of Spitsbergen (Svalbard). *Acta Palaeobotanica* 47: 89–107.
Upchurch GR Jr., Otto-Bliesner BL, and Scotese CR (1999) Terrestrial vegetation and its effects on climate during the latest Cretaceous. In: Barrera E and Johnson CC (eds.) *Evolution of the Cretaceous Ocean-Climate System*. Special Paper 332. Boulder, Colorado: Geological Society of America.
Urey HC, Lowenstam HA, Epstein S, and McKinney CR (1951) Measurement of paleotemperatures and temperatures of the upper Cretaceous of England, Denmark, and the southeastern United States. *Bulletin of the Geological Society of America* 62: 399–416.
Vail PR, Mitchum RM Jr., and Thompson S III (1977) Global cycles of relative changes of sea level. In: Payton CE (ed.) *Seismic Stratigraphy and Global Changes of Sea Level*, pp. 83–97. American Association of Petroleum Geologists Memoir.
Valdes PJ (2000) Warm climate forcing mechanisms. In: Huber BT, et al. (ed.) *Warm Climates in Earth History*, pp. 3–20. Cambridge, UK: Cambridge University Press.
Van der Gracht WAJMvW (1931) Permo-carboniferous orogeny in the south-central United States. *American Association of Petroleum Geologists Bulletin* 15: 991–1057.
Wagner F, Neuvonen S, Kürschner WM, and Visscher H (2000) The influence of hybridization on epidermal properties of birch species and the consequences for palaeoclimatic interpretations. *Plant Ecology* 148: 61–69.
Wallmann K (2001) Controls on the Cretaceous and Cenozoic evolution of seawater composition, atmospheric CO_2 and climate. *Geochimica et Cosmochimica Acta* 65: 3005–3025.
Weijers JWH, Schouten S, Sluijs A, Brinkhuis H, and Sinninghe Damsté JS (2007) Warm Arctic continents during the Palaeocene–Eocene thermal maximum. *Earth and Planetary Sciences Letters* 261: 230–238.
Weissert H and Lini A (1991) Ice age interludes during the time of Cretaceous greenhouse climate. In: Müller DW, McKenzie JA, and Weissert H (eds.) *Controversies in Modern Geology*, pp. 173–191. London: Academic Press.
Wilf P (2000) Late Paleocene–early Eocene climate changes in southwestern Wyoming: Paleobotanical analysis. *Geological Society of America Bulletin* 112: 292–307.
Wilf P, Cúneo NR, Johnson KR, Hicks JF, Wing SL, and Obradovich JD (2003) High plant diversity in Eocene South America: Evidence from Patagonia. *Science* 300: 122–127.
Wilf P, Wing SL, Greenwood DR, and Greenwood CL (1998) Using fossil leaves as paleoprecipitation indicators: An Eocene example. *Geology* 26: 203–206.
Wilson PA and Norris RD (2001) Warm tropical ocean surface and global anoxia during the mid-Cretaceous period. *Nature* 412: 425–429.
Wilson PA, Norris RD, and Cooper MJ (2002) Testing the Cretaceous greenhouse hypothesis using glassy foraminiferal calcite from the core of the Turonian tropics on Demerara Rise. *Geology* 30: 607–610.
Wilson PA and Opdyke BN (1996) Equatorial sea-surface temperatures for the Maastrichtian revealed through remarkable preservation of metastable carbonate. *Geology* 24: 555–558.
Wing SL, Harrington GJ, Smith FA, Bloch JI, Boyer DM, and Freeman KH (2005) Transient floral change and rapid global warming at the Paleocene–Eocene boundary. *Science* 310: 993–996.
Wolfe JA (1978) A paleobotanical interpretation of Tertiary climates in the northern hemisphere. *American Scientist* 66: 691–703.
Wolfe JA (1980) Tertiary climates and floristic relationships at high latitudes in the northern hemisphere. *Palaeogeography, Palaeoclimatology, Palaeoecology* 30: 313–323.
Wolfe JA (1994) Tertiary climatic changes at middle latitudes of western, North America. *Palaeogeography, Palaeoclimatology, Palaeoecology* 108: 195–205.
Yapp CJ and Poths H (1992) Ancient atmospheric CO_2 pressures inferred from natural goethites. *Nature* 355: 342–344.
Zachos JC, Dickens GR, and Zeebe RE (2008) An early Cenozoic perspective on greenhouse warming and carbon-cycle dynamics. *Nature* 451: 279–283.
Zachos JC, Opdyke BN, Quinn TM, Jones CE, and Halliday AN (1999) Early Cenozoic glaciation, Antarctic weathering, and seawater $^{87}Sr/^{86}Sr$: Is there a link? *Chemical Geology* 161: 165–180.
Zachos J, Pagani M, Sloan L, Thomas E, and Billups K (2001) Trends, rhythms, and aberrations in global climate: 65 Ma to present. *Science* 292: 686–693.
Zachos JC, Röhl U, Schellenberg SA, et al. (2005) Rapid acidification of the ocean during the Paleocene–Eocene thermal maximum. *Science* 308: 1611–1615.
Zachos JC, Schouten S, Bohaty S, et al. (2006) Extreme warming of mid-latitude coastal ocean during the Paleocene–Eocene thermal maximum: Inferences from TEX_{86} and isotope data. *Geology* 34: 737–740.
Zachos JC, Stott LD, and Lohmann KC (1994) Evolution of early Cenozoic marine temperatures. *Paleoceanography* 9: 353–387.
Zeebe RE (1999) An explanation of the effect of seawater carbonate concentration on foraminiferal oxygen isotopes. *Geochimica et Cosmochimica Acta* 63: 2001–2007.

Zeebe RE (2001) Seawater pH and isotopic paleotemperatures of Cretaceous oceans. *Palaeogeography, Palaeoclimatology, Palaeoecology* 170: 49–57.
Zeebe RE, Zachos JC, and Dickens GR (2009) Carbon dioxide forcing alone insufficient to explain Palaeocene–Eocene thermal maximum warming. *Nature Geoscience* 2: 576–580.
Zhang Z, Nisancioglu KH, Flatøy F, Bentsen M, Bethke I, and Wang H (2011) Tropical seaways played a more important role than high latitude seaways in Cenozoic cooling. *Climates of the Past* 7: 801–813.
Zhang X, Zwiers FW, Hegerl GC, et al. (2007) Detection of human influence on twentieth-century precipitation trends. *Nature* 448: 461–465.
Zhou J, Poulsen CJ, Pollard D, and White TS (2008) Simulation of modern and middle Cretaceous marine $\delta^{18}O$ with an ocean–atmosphere general circulation model. *Paleoceanography* 23: PA3223.
Ziegler AM, Eshel G, Rees PM, Rothfus TA, Rowley DB, and Sunderlin D (2003) Tracing the tropics across land and sea: Permian to present. *Lethaia* 36: 227–254.